Development of PV panel recycling process enabling complete recyclability of end-of-life silicon photovoltaic panels

Pradeep Padhamnath[1*], Srinath Nalluri[2], Filip Kuśmierczyk[1], Mateusz Kopyściański[1], Joanna Karbowniczek[1], Tomasz Kozieł[1], Leow Shin Woei[2], Thomas Reindl[2].

[1]AGH University of Krakow, al. Adama Mickiewicza 30, 30-059 Kraków, Poland

[2]Solar Energy Research Institute of Singapore, 7 Engineering Drive 1, National University of Singapore, Singapore 117574

* ppadhamnath@agh.edu.pl

Abstract

The cumulative PV panel waste is expected to reach ≈ 8 million tonnes by 2030 and ≈80 million tonnes by 2050. This presents an opportunity to pursue new avenues in terms of recycling and improving the circularity of the PV panels. In this work we present experimental results for recycling c-Si PV panels using recently developed electrohydraulic shock-wave fragmentation (EHF) of PV panels. The EHF process allows for the recovery of all materials used in the manufacturing of PV panels. We use different types of panels for the recycling process and analyse the material recoverability in each condition. Further, we analyse the effectiveness of chemical treatment in isolating metals from the silicon obtained from recycled c-Si PV panels, providing an opportunity of recovering high quality metal and silicon. The separation process allows for the high-quality material recovery and could potentially improve the economic feasibility of the overall recycling process.

1.Introduction

The global growth of solar photovoltaic (PV) installations since the early 2000s has been extraordinary, increasing from 1.2 GW in 2000 to 1.6 TW in 2023, with projections suggesting it will reach 4.5 TW by 2050 [1–3]. Solar energy is thus expected to become the most dominant source of electricity generation. While this exponential growth is a crucial and desirable step in addressing climate change, challenges arise in managing decommissioned solar panels. PV panels have a technical lifespan of 25 to 30 years; however, some fail prematurely due to damage during production, transportation, installation, or field degradation. Thus, as PV installations increase, global cumulative PV waste is also projected to grow exponentially, reaching up to 8 Mt by 2030 and 78 Mt by 2050, with annual waste in 2050 (6 Mt) almost matching the mass contained in new installations (6.7 Mt) [4]. Hence, it has become imperative for many companies to integrate PV recycling into the PV value chain to mitigate growing PV waste, ensure the technology remains environmentally friendly and sustainable, and to create value by pursuing new economic avenues.

However, recycling end-of-life (EOL) photovoltaic (PV) modules or panels is extremely challenging due to the complex structure of the panels. Crystalline silicon (c-Si) panels, which represent about 97% of the market [5], are made from a variety of materials—including glass, interconnected cells which have doped silicon, and metals like aluminium, silver, and copper,

encapsulants, and polymers—all laminated together in heat and pressure to form a single structure. This intricate composition requires a range of mechanical, thermal, and chemical methods to disintegrate the layers, recover all the useful materials and purify them for reuse[6]. Research and development in PV recycling technologies have made significant strides in recent years. Between 1995 to 2016, there were around 123 effective patents from various countries related to the recycling of c-Si PV panels, highlighting the increasing demand and necessity of PV recycling. Europe has pioneered PV panel recycling, with PV Cycle leading efforts since 2001, successfully processing over 19 Mt of PV waste. Innovations included processes combining mechanical and thermal treatments to increase recycling rates to 96%. In Germany, Eltz Umwelt-Technology devised an advanced pyrolysis process to recover 95% of materials. France's Veolia utilizes a multistage recycling approach for high-efficiency recovery. China leads in PV patents, focusing on panel separation, with innovative technologies like refrigerated grinding and hydrothermal prefractionation. In Japan and Korea, technologies like heated cutting and thermal treatment are advancing PV recycling efficiency[7]. Thus, globally there has been increased demand for advanced PV Recycling technologies. Despite the technical feasibility and the advancements, recycling of PV panels often face environmental and economic challenges, including harmful emissions from incineration and the use of toxic chemicals during leaching, coupled with high operational costs and limited waste volumes that prevent economies of scale[8]. Hence, the focus is being shifted towards creating sustainable, cost-effective and large-scale technologies to promote the long-term viability of solar energy. To extract valuable materials from the end-of-life PV panels, usually four steps are required – disassembly, delamination, material sorting and material extraction. Each of these steps could further comprise single or multiple process steps [9,10]. The external wiring (copper) and the aluminum frames are easily extracted and recycled or in some cases reused entirely [11]. In some cases, commercial recycling of PV panels could only include these steps, while discarding the remaining unframed panels or PV laminates [10]. Metals, notably Ag, Cu and Al are among the most valuable recyclable component in a PV panel followed by Silicon. The polymers such as Ethylene-vinyl acetate (EVA), polyvinylidene difluoride (PVDF) and Polyethylene terephthalate are almost never recycled, owing to their lower economic value and hazardous nature of recovery process [9,12–14]. The recent progress and the state of the art in the PV panel recycling has been extensively covered in these reviews [9,15–24]. Hence, we shall only present succinct overview of the development of the process and the current status regarding recovery of Ag and Si which are among the most valuable and most difficult materials to recover from an EOL c-Si PV panel. Further we present a short overview of the delamination processes used in the recycling of PV modules as a segue to the main experimental process used in this work.

1.1 Recovery of Silver from EOL PV panels

In c-Si PV panels, electrons generated in the silicon wafer are collected through a grid-patterned contact printed on the cells, which is typically made of silver paste. While the silver content in the PV panel is minimal by weight (~0.05%), it accounts for 47% of the overall cost in terms of 'value standpoint'[6,25]. Furthermore, the shift in the photovoltaic (PV) industry from Passivated Emitter and Rear Cell (PERC) to newer technologies like Tunnel Oxide

Passivated Contact (TOPCon) and Heterojunction Technology (HJT) is driving an increase in silver usage, with TOPCon utilising at least 1.3 times and HJT utilising at least 1.6 times more silver than PERC. According to the World Silver Survey 2023 by The Silver Institute, as demand rises amidst tight supply, silver consumption in PV panels is projected to grow by 4%, while production is forecasted to increase by only 2%, resulting in PV industry exhausting up to 98% of the global silver reserves in 2050 [26]. Therefore, inclusion of effective recovery of silver into the recycling line of PV panels is very much vital to enhance the cost viability of the entire recycling process, offset the production costs of new panels as well as meet the growing demand of silver.

In the early days of PV recycling plants, the primary goal was high-volume material recycling to glass, aluminium, and silicon as it made up over 80% of panel mass, simpler to separate and cost-effective because of established recycling markets. Furthermore, recovery of intact solar cells for reuse in panel production was prioritised, as the price of PV panels was largely driven by the cost of silicon wafers [7]. Consequently, silver was discarded during the etching of solar cells in sodium hydroxide to recover silicon, as it was considered uneconomical to retrieve trace amounts of silver, despite its high value. Recovering silver from PV panels kickstarted only in 2000s and the common technique used was hydrometallurgical processes. Chemicals like nitric acid were used to leach metals from the recovered solar cells. The silver which is dissolved in the nitric acid is precipitated as a salt and silver is recovered from it through electrolysis and metal replacement techniques [27]Around 99% silver could be recovered through these processes.

Researchers have developed more efficient methods in recent years. For instance, a combined hydrometallurgical and electrochemical approach has been shown to achieve a 98% recovery rate. This process employs leaching followed by electrodeposition-redox replacement (EDRR) to recover pure silver, offering high efficiency and environmental advantages by minimizing chemical use[28]. Another promising method is laser debonding, where silver electrodes are removed using laser techniques. This method has been explored by the University of Virginia and has shown potential for selectively recovering silver while preserving the integrity of the silicon wafers. The laser method also generates silver nanoparticles, which are valuable for reuse in various industries. The use of machine learning to optimize laser processing is an innovative trend aimed at automating and scaling the recovery process, reducing both cost and energy consumption[29]. Recent advancements have focused on increasing the recovery efficiency while reducing the environmental footprint of the recycling processes. For example, research has shown that using iron and aluminium chloride in brine solutions can recover up to 95% of silver in under 10 minutes. This method is touted for its low cost, low toxicity, and scalability compared to conventional acid-based recovery techniques[30]. Despite these advancements, several challenges persist in silver recovery from PV panels. One significant issue is the low concentration of silver in PV cells, which can make the recovery process economically unviable at scale. The cost of extraction is often high due to the need for complex chemical processes or specialized equipment such as lasers. Additionally, the presence of other metals, such as copper, which have similar chemical properties, complicates the leaching and separation processes[28]. The development of

methods that can selectively recover silver without affecting other valuable materials, such as silicon, remains a technological hurdle. While traditional hydrometallurgical techniques are being optimized for higher efficiency, novel methods such as laser debonding and electrochemical recovery offer promising avenues for enhancing sustainability in the PV industry. However, challenges related to the economic viability of recovery and the low silver content in panels must be addressed to scale these technologies effectively.

1.2 Recovery of Silicon from EOL PV panels

Researchers have demonstrated the prospects of reusing the silicon recovered from end-of-life Si PV panels to manufacture new silicon solar cells. Silicon recovered after the usual recycling process involving crushing and separating is usually metallurgical grade [7,31,32] , which is valued around $2-3/kg depending on the region [33]. There could be motivation to recover solar grade silicon, which is valued between $6-9/kg [34]. Closed loop recycling of Si in the solar industry has been reported to be feasible [32]. Researchers have used the recycled silicon from broken solar cells and wafer production to fabricate ingots and subsequently solar cells [35]. The recycled solar cells achieved efficiency of 18.1% compared to a reference of 18.5%. Recently, researchers fabricated solar cells with efficiencies exceeding 20% from recycled silicon, obtained after chemical etching [36]. Researchers have demonstrated the effectiveness of etching process in removing metal contamination from silicon [37–39]. Among the earliest attempt of recovering silicon, researchers used thermal delamination and chemical etching using a combination of HCl, HF and NaOH to recover 62% of the Si of 8N quality from the EOL PV panels [40]. Using a slightly different chemicals, such as HF, HNO_3, H_2SO_4 and CH_3COOH, researchers recovered 79-86% of 5N silicon, using chemical delamination process to remove the glass and the polymers [41]. Park et.al fabricated single cell panels and used thermal delamination to remove the glass and the EVA layers [38]. By using HNO_3 and KOH, they were able to recover 90% of the silicon, in the original size of the wafer (albeit thinner). These reclaimed wafers were used to make solar cells, which achieved ≈90% of the original efficiency [38]. Similar approach to remove metal using HNO_3, H_3PO_4 and KOH was used to recover 80-90% of the silicon [31,42–45]. By recycling solar cells rejected during production, which have not been incorporated in a panel, researchers were able to retrieve ≈ 99% of the silicon [46]. For this advanced process such as ultrasonic treatment, centrifugal separation and microfiltration were employed. The succinct literature review presented here demonstrates the underlying interest in recycling silicon from the solar cells and the complicated process required. In all the instances, silicon was recovered by employing either a thermal or a chemical delamination process. Nevertheless, it has been established that silicon recovered from EOL PV panels could be reused for fabricating new solar cells.

1.3 Delamination of EOL PV modules

Delamination is among the most complicated steps which is crucial to the recovery of high-quality materials from the PV panels. The long-term performance of the PV panels is dependent on their ability to withstand environmental impacts such as ingress of moisture and air. Therefore, great care is exercised in laminating PV panels, thereby rendering delamination of the panels a difficult task. PV panels can be delaminated using mechanical, chemical or thermal

processes, or a combination of them. To achieve delamination using thermal route, the PV panels are heated to temperatures in the range of ≈450-550°C which decomposes the cross-linked polymers such as Ethyl Vinyl Acetate (EVA), Polyvinylidene fluoride (PVDF) or polyethylene terephthalate (PET) [47]. This separates the glass, the interconnecting metallic ribbons and the solar cells, and allows subsequent recovery of high-quality materials [37,48–50]. Energy consumption and generation of toxic gases makes this process expensive to implement [15,51–53]. Chemical delamination of modules is performed by treating the panels (in their entirety) or after mechanical crushing, in organic or inorganic chemicals which can dissolve the cross-linked polymers, thereby enabling the separation of the laminated panels, and partially cleaning the glass in the process. This process usually involves extremely hazardous chemicals and long process times, sometimes extending more than 10 days [9,10,15]. Researchers have combined chemical treatment with microwaves [54], ultrasonic waves [55] or supercritical carbon dioxide [56] to shorten the process durations. In some cases, complete separation of EVA and PET/PVDF was not always achieved, and secondary treatment such as pyrolysis or glycolysis was necessary [57]. Furthermore, disposal of such large scale of organic chemicals could be environmentally challenging.

Mechanical fragmentation techniques are the most widely reported and used approach for recycling PV panels [7,58]. Shredding, crushing, milling and grinding have been used for fragmentation of PV panels [59,60]. Some other processes of mechanical separation include using a hot knife to separate the glass panels [7,61–64] and mechanical peeling after heating the modules to a temperature sufficient enough to melt the polymer layers [65,66].

Recently delamination of end-of-life PV panels using high voltage crushing or electrohydraulic fragmentation (EHF) has gathered attention of the researchers as an excellent alternative to the existing delaminating processes for achieving higher recycling efficiency and material selectivity than conventional crushing [67–71]. Its principle of operation includes applying a high voltage pulse to a solid immersed in a fluid to generate a shockwave. The shockwave travels through the fluid and interacts with the solids, causing fractures at the weak points between the interfaces of different materials, along with crushing of the material[67]. The material recovered after the fragmentation usually consists of fine powder containing metals and silicon from the solar cells, along with glass powder [68,69]. EHF has been shown to be better suited for recovery of metals (Al, Ag) and Si from the PV panels [70] as well as extremely energy efficient [68]. While the process parameters have been optimized by the researchers, they have been limited to the parameters of the process chamber. Data regarding the relationship of feed material and their impact on the process is not sufficient in the published literature.

In this work, we present the effectiveness of newly developed EHF process in recycling different types of silicon PV panels, such as glass-glass, glass-backsheet and glass-free panels. The panels are cut into regular shapes and fed into the EHF processing chamber. Water is used as the fluid medium for this process. We investigate the effect of the feed size and process duration on the material recovery from the process, both qualitatively and quantitatively. We design and present step-by-step processes to remove and recover metals (Al and Ag), high quality silicon and polymers from the recycled PV panels. We demonstrate that EHF process

is capable of recycling the PV modules entirely. We employ chemical recovery methods to recover metals and purify silicon, generating commercially important gas in the process. Through the investigations presented in this work, we demonstrate the suitability of the EHF process in recycling c-Si PV panels.

2. Experimental Details

2.1 Fabrication of solar cells and panels

The PV panels used in this work along with metallized wafers used for fabricating the panels were all fabricated in the laboratory. The panels were prepared with metallized samples using a process similar to that used for preparing the solar cells, however functioning solar cells were not fabricated. For making the PV panels, bi-facial samples (featuring H-type metal grid on both front and rear sides) were prepared. The dummy wafers were prepared using large area (M2) boron doped (p-type) Cz wafers. The wafers were first saw damaged etched in potassium hydroxide (KOH) solution (20%wt, 80 ◦C) followed by standard Radio Corporation of America (RCA) cleaning process [72]. The wafers were textured using the standard alkaline (KOH) based texturing process. The wafers were doped with Phosphorus using high temperature diffusion process using $POCL_3$ as the dopant gas. After the diffusion, the phosphosilicate glass was removed by dipping the wafers in HF (10%) solution at room temperature. The diffusion was performed to allow for the contact formation during the metallization process [73]. Further, the etch rate of the Si is known to depend on the level of dopant [74–76], hence, doping the silicon was done to mimic the interaction with the chemicals of functioning solar cells. The wafers were coated with silicon nitride on both sides to act as the antireflection coating (ARC) in an inline plasma enhanced chemical vapour deposition tool. The wafers were metallized with H-pattern using an inline industrial screen-printer. The ‘front side’ featured 83 fingers, and five bus bars printed with an Ag paste. The ‘rear side’ featured 110 fingers, and five bus bars printed with a fire-through Al paste. The samples were fired at high temperature (750°C) to allow the metal to form contacts to the Si substrate, as in actual solar cells.

Three types of panels were prepared for determining the effectiveness of the electrohydraulic delamination process in separating the components of the PV panels. Glass-Glass (GG) panels had layer of glass on both sides, with ethylene-vinyl-acetate (EVA) copolymer-based layer as the encapsulant. Glass-Backsheet (GB) panels had glass on the front and polyethylene terephthalate (PET) based backsheet on the rear, with EVA as the encapsulant. Glass-free panels had PET based transparent front sheets (fs) on the front and opaque backsheet (bs) on the rear with EVA as the encapsulant. Every panel was prepared with 60 metallized samples on an industrial inline stringer machine. The samples were stringed using 0.9mm Cu ribbons to form a string of 10 samples. Six such strings were cross connected (soldered) using 5mm tin-coated copper connector. A layer of EVA sheet was placed on the front glass sheet, over which the stringed wafers were placed. This was followed by a second EVA layer for encapsulation and finally the second glass sheet was placed on the top. The thickness of the glass panel used in this work was 3mm. The panel was then transferred to laminator where it was heated to 150°C, in vacuum for 10 min followed by 10 minutes annealing with an application of 800 mBar of pressure. Similar process was used for glass-backsheet panel where the second layer of glass

was replaced by the white PET based backsheet (0.275 mm). For glass-free panels, a PET based transparent sheet (0.275 mm thick) was used on the front while the PET based white backsheet was used as the rear side. The laminating process was kept same for all the panels. All the modules were stored in a wooden container for a period between three-four months before being used for experiments. Fig 1 shows the cross-section images of the fabricated PV panels.

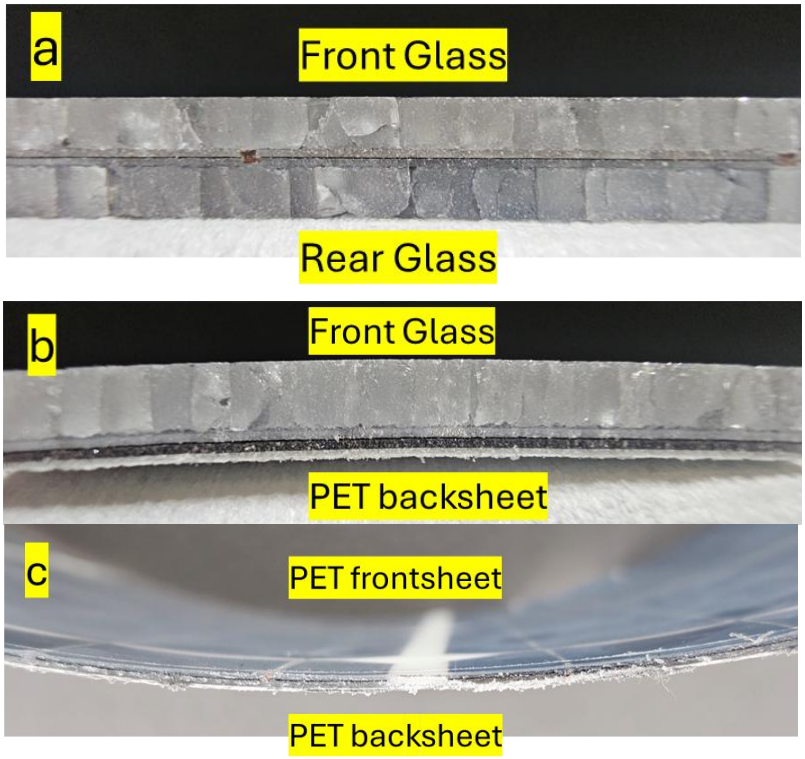

Figure 1- Cross sections of the three types of PV panels prepared in this work a) glass-glass (GG) b) Glass-backsheet (GB) and c) Glass-free (GF)

2.2 Electrohydraulic Fragmentation technology

The electrohydraulic fragmentation method has been proposed as an alternative to the thermal or chemical processing of PV panels [67–70]. This process allows for room temperature separation, extraction and recovery of the materials from end-of-life c-Si PV panels, without generation of toxic wastes. In this process, a high-pressure pulse propagating through a suitable liquid medium, such as water, is used for the fragmentation of the PV panels. Figure 2 shows the concept of electrohydraulic fragmentation process.

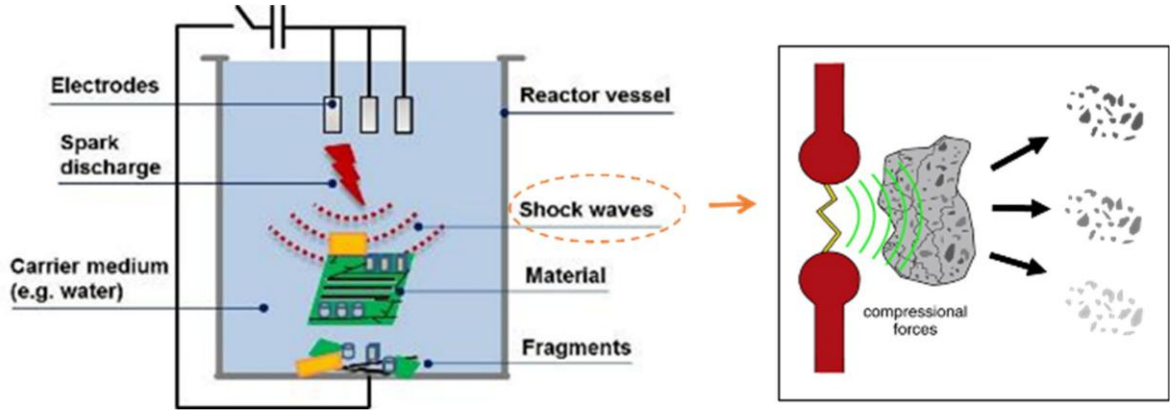

Figure 2: Process schematic of the electrohydraulic fragmentation technique.

The electrohydraulic fragmentation technique relies on the shockwaves due to arcing between electrical electrodes suspended in a liquid medium, such as water. The electrical electrodes are connected to a power supply of ≈ 50 kV. The shockwaves generated as a result of the arcing, propagate through the liquid medium and interact with PV panel immersed in the liquid. The use of this technology is directed towards recovering the materials from the laminated portion of the PV panel which includes front glass layer, solar cells, encapsulants and backsheet or glass for monofacial or bifacial panels respectively. The Al frame, the external junction box and wires are already removed using a simple mechanical separation process before the laminated portion of the panel is immersed in the chamber. The PV panels after this process are referred to as laminated PV panels throughout this work. The electrical arcing generated shockwaves in the fluid medium [67,69]. Interaction of shockwave and the immersed laminated PV panels results in the disintegration of the composite panel into individual materials based on the differences in acoustic properties and mechanical strength. After the disintegration in the fragmentation unit, the individual materials (i.e. glass, backsheet, EVA, Cu ribbons and solar cells) are separated by filtration, sorting and binning as they pass through though different sieves. The materials obtained can be further recycled to extract Si and Silver through downstream chemical processes, while the glass, copper/aluminium/silver contacts can be reused post purification and melting. A significant advantage of this process is the recovery of the various polymers used in the PV panel, such as EVA and polymer backsheet which can be recycled. In pyrolysis process these polymers are burnt and lost, generating toxic fumes in the process. Hence, this process provides a cleaner and less energy intensive alternative to recover materials from the PV panels leading to almost complete circularity (≈99% by wt.) of the PV panels.

Three different types of panels, glass-backsheet, glass-glass and glass free panels were fabricated to test the adaptability of the process. The panels were fabricated in our lab using the standard process. The laminated PV panels were cut into sizes using a high-pressure water jet into two different sizes which were used as feed material for the batch process chamber.

3. Experimental results and discussions

3.1 Material recovery using the water jet cutting process.

The laminated PV panels were cut into smaller pieces using a high-pressure water jet. To understand the impact of the size of the feed material on the material recovering efficiency, the laminated panels were cut into square pieces of two different sizes. Fig 3 shows the panel cutting process using water jet. In each process run, similarly sized pieces obtained from the same type of panel were fed into the process chamber. After electrohydraulic processing for 240 seconds, the materials were recovered from the chamber, dried and then segregated into different sizes using a manual sieving process.

Figure 3: A glass-backsheet laminated PV panel being cut using the water jet cutting process.

Fig 4 shows the materials recovered after processing the glass-glass panels pieces. The polymer layers were not damaged by water pressure and were recovered as pieces approximately in the size they were originally cut using the water jet. While most of the silicon and metal present in the form of solar cells were separated from the EVA layers, a fraction of the solar cells was still found attached to the polymer layers, especially EVA, in the glass-glass and glass free PV panels. In the case of glass-backsheet PV panels, the front EVA was separated from the solar cells while the rear EVA and PET backsheet remained stuck together, along with some remnants of the silicon solar cells. Recycled glass was mainly obtained as pieces (≈1-5 mm) and coarse powder (≈ 0.25-1 mm) while finer glass, silicon and metal particles were obtained as fine powder (≈ <0.25 mm). Copper ribbons and cross connectors used for interconnection were also obtained in their whole form.

Figure 4: Recovered material after recycling a glass-glass panel using electrohydraulic processing a) Sieving and sorting the materials recovered b) the sorted materials recovered after drying.

310

311 **3.2 Effect of different process parameters on material recovery**

312 Figure 5 shows the relative percentage of different materials recovered from the different types
313 of panels for a feed size of 2.5cm x 2.5 cm^2 for all panels and processing duration of 240s.

314 Measured quantity of the pieces from different panels were fed into the chamber and the
315 recovered materials were dried and measured again. The experiment was repeated in five
316 batches for each type of panels (total of 15 runs). The weight of each type of panel used for
317 each process run for the experiment were ≈100g for GF panels, ≈200g for GB panels and ≈450
318 g for GG panels. The difference in weight was due to the difference in the density of the
319 respective panels. However, similar volume of the batch process container was occupied during
320 each process run. The optimal weight of the pieces of the panel and the volume of the process
321 chamber was optimized separately. It was observed that the efficiency of separation initially
322 increased with the increasing weight and reached a maximum, beyond which it started to
323 decline. For example, for glass backsheet panels, the cleanest EVA sheets were obtained for a
324 feed of 200g per run. For both 100g and 400g of feed, the separation of the materials was
325 suboptimal, with more silicon covering the polymer surface, indirectly implying a lower
326 percentage of recovered powdered silicon. This process was repeated for each panel and the
327 optimal weight of the feed material was determined. This is important because more feed
328 material than optimal could clog the filters and damage the internal components. More number
329 of pieces could also lead to constrained motion of the pieces in the fluid and hinder proper
330 interaction with the pressure pulse.

331 The weight of the materials (dried) recovered from all types of PV panels was ≈99%, signifying
332 the high material recovery efficiency of the process. The materials recovered were classified in
333 five categories – pieces of polymers (EVA, front and backsheet), interconnecting metal ribbons,
334 glass pieces (>2 mm), coarse powder (1-2 mm) and fine powder (< 1 mm). Coarse powder
335 comprised glass and silicon pieces, while fine powder mostly included silicon and metal.

Furthermore, the polymer recovered were either separated or joined with other polymers. For example, in glass-backsheet panels, the EVA was obtained on its own as well as attached to the backsheet. In glass-free panels, the polymers included pieces of front sheet, EVA and EVA +backsheet stuck together. Figure 6 shows the different components of the polymer recovered after the recycling process.

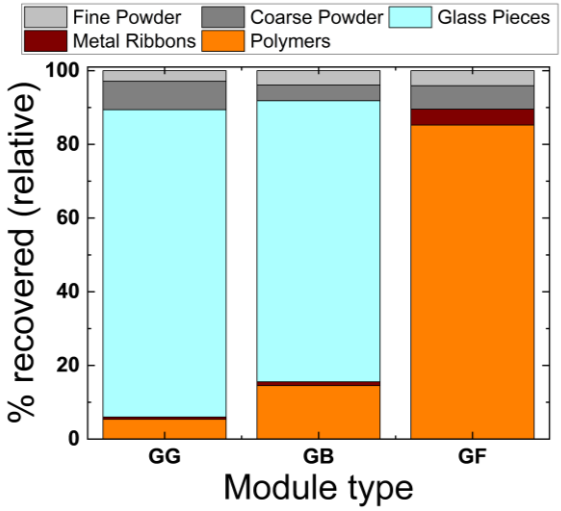

Figure 5: Material recovered for different types of panels when the feed size and processing times are kept similar.

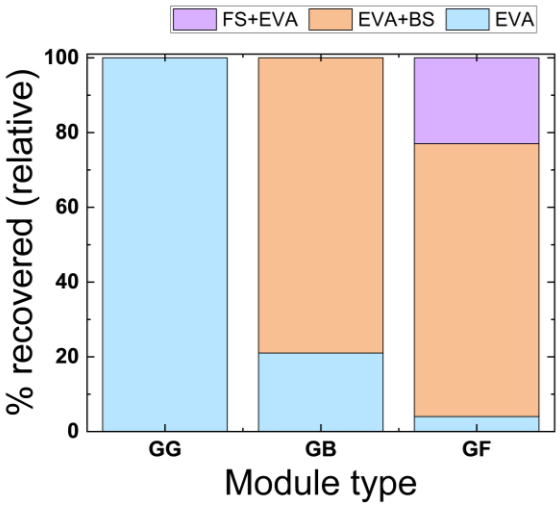

Figure 6: Breakdown of the polymer particles recovered from the different types of panels when the feed size and processing times are kept similar.

From the experiments it was found that the glass-glass panels were easily and quickly separated and yielded high quality yield. In the absence of the backsheet, >90% of the constituents were separated and recovered as single material (glass, ribbons, EVA). The water pulse is most effective in separating materials with different mechanical properties. In the absence of front/rear sheets in the glass-glass panels, the encapsulant (EVA) is attached to the glass on both front and rear sides. Hence, the dissimilarity of the mechanical properties of the material at the interface allowed for the efficient separation and subsequent recovery of the EVA during the recycling process. Furthermore, the EVA obtained from the glass-glass panels were the cleanest and had least amount of Si sticking to the EVA surface. In glass-backsheet panels, the EVA on the front was separated and recovered as a single layer. The EVA bonded with the backsheet could not be separated and all pieces of backsheet has some EVA stuck to them. It was also observed that in these panels, the only EVA pieces were relatively cleaner and had less silicon pieces sticking to them than the EVA-backsheet combined pieces. The glass free panels were the most difficult to recycle and only 4% of the total weight of the polymer recovered comprised only EVA pieces. This can be attributed to the strong bonding strength between the different polymer layers and the similarity in their mechanical properties. Additionally, more silicon remains were found on the EVA-backsheet pieces. Hence, for glass free panels, the separation was least efficient in terms of quality of the materials retrieved.

Table 1 shows the two different sizes into which the panels were cut using the water jet process.

Table 1: Table showing the two different sizes into which the panels were cut using the water jet cutting process. All dimensions are in cm.

PV panel Type	Size 1 (S1)	Size 2 (S2)	Process duration (s)
Glass-Glass (GG)	2.5x2.5	5x5	240, 480, 720
Glass-Backsheet (GB)	2.5x2.5	5x5	
Glass-Free (GF)	2.5x2.5	5x5	

Table 2 shows the process yield in relative percentages for the different processing conditions employed in the experiment. Each data showed in the table is the average of three individual experiments. The process yield was calculated by weighing the material recovered after drying and is presented as a percentage of the weight of the material fed into the process.

Table 2- Impact of process parameters on the yield of the recycling process. The yield of individual components is expressed in percentage of the total process yield.

Panel type	Feed size [cm^2]	Process duration	Process Yield [%]	Polymers [% wt.]	Metal Ribbon [% wt.]	Glass Pieces [% wt.]	Coarse Powder [% wt.]	Fine Powder [% wt.]
GG	2.5x2.5	240	98.8	05.37	0.6	83.44	07.71	02.88
GG	2.5x2.5	480	98.5	05.22	0.6	73.70	09.13	11.35
GG	2.5x2.5	720	98.4	05.13	0.69	61.29	11.46	21.43
GG	5x5	240	98.9	05.46	0.61	84.92	07.57	01.44
GG	5x5	480	98.8	05.30	0.67	74.01	08.66	11.36
GG	5x5	720	98.6	05.15	0.55	69.73	09.68	14.89
GB	2.5x2.5	240	98.8	11.50	1.04	76.29	05.26	05.91
GB	2.5x2.5	480	98.8	11.17	1.07	73.19	06.37	08.20
GB	2.5x2.5	720	98.7	10.38	0.99	67.29	06.68	14.66
GB	5x5	240	98.9	11.34	1.10	77.22	04.24	06.10
GB	5x5	480	98.8	10.57	1.27	71.59	05.43	11.14
GB	5x5	720	98.7	10.87	1.52	70.03	04.40	13.18
GF	2.5x2.5	240	99.2	87.75	3.42	0	06.17	02.66
GF	2.5x2.5	480	98.8	83.81	4.23	0	07.16	04.80
GF	2.5x2.5	720	98.5	81.55	6.60	0	06.18	05.67

The yield for all the processes was ≈ 99%. Although maximum precautions were exercised, for example flushing the equipment after each run, the crossing over of a tiny portion (≈1%) of yield from one experiment to another cannot be denied. Furthermore, the material recovery could be improved by employing filtering under pressure which was beyond the scope of this work. Additionally, the fine powder sticking to the surface of the container and the internal parts of the chamber could not be completely recovered. The yield decreases slightly with increasing processing time, probably due to the higher fraction of non-recoverable fine powder. The experimental data showed that both time and size of the feed material, in addition to the panel type, impacted the process yield. For glass free panels, pieces of size 5x5 cm^2 could not be separated effectively for any process duration. This was probably due to the fact that in larger pieces, there were regions where the front and rear polymer layers were bonded encasing

the solar cell within. These layers, due to the similar mechanical properties could be separated. Only few pieces where the solar cells were exposed at the edges on all sides were able to separate, even then the separation was not clean. Therefore, for the glass-free panels the data is limited to 2.5x2.5 cm^2 size of the feed material. For all other panel types, the feed size did not have a significant quantitative impact on the process yield. However, when the size of the feed material was smaller, the polymer pieces obtained after recycling process were cleaner with lower content of silicon particles (from the solar cells) sticking to them. Smaller pieces are expected to move around the chamber more easily and have higher probability of getting impacted by the shockwaves and getting separated.

Process duration was shown to have a clear impact on the quality of yield and the quantity of the individual components recovered after the recycling process. With the increase in the process duration, fraction of glass pieces decreased with increase in both coarse and fine powder content. This is expected as with the increase in process duration, more shockwaves impact the PV panel pieces. The increase in the number of shockwaves leads to increased crushing of the materials such as glass and silicon solar cells and hence, the yield has higher percentage of coarse and fine powdered material. It was also observed that the percentage of fine powdered material in the yield increases significantly, across the panel types and size of the feed material. The relative yield of fine powder was generally higher for smaller feed material as compared to the larger size of feed material for the same panel type. The increase in quantity of powder could primarily result in increased content of glass in powder form, as it disintegrates under the impact of the shockwaves. The impact of the prolonged process duration was clearly visible on the EVA films recovered after the process. Longer process duration resulted in higher proportion of EVA in the recovered polymer. Hence, it can be deduced that longer process duration led to higher separation of the EVA from the backsheet or the first sheet. Further. the longer duration of processing resulted in clear EVA films with minimal amount of silicon sticking to the polymer's surface. Figure 7 shows the pieces of EVA recovered post treatment of the glass-glass panels for different process durations. It can be clearly seen that the longer process duration results in cleaner EVA sheet and higher quality recovery of the materials, including silicon. This was also observed in the experimental data where the weight percentage of the polymer recovered decreased slightly with increasing processing duration for the same feed size and panel type. For example, for glass-glass panels, the weight fraction of EVA decreases by 0.3% when the process duration was increased from 240s to 720s for 5x5 cm^2 samples. The decrease in the weight fraction of the polymer was also found to be dependent on the size of the feed material. For example, for glass-backsheet panels, when the process duration was increased from 240s to 720s, the weight fraction of the polymers decreased by ≈2.1% for 2.5x2.5 cm^2 pieces, while it decreased by ≈ 3.5% for 5x5 cm^2 pieces. This implies that bigger feed material might need longer process duration to obtain a good quality of separation and recovery of clean polymers. However, the increased duration could also increase the amount of glass in the powder form. To avoid this, big pieces of glass could be separated by a screening and filtering mechanism in between the shock treatments.

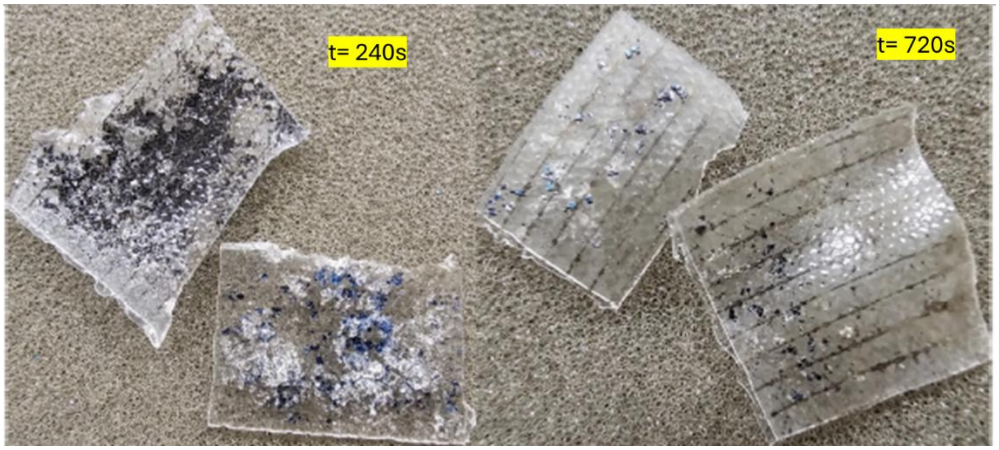

Figure 7: EVA pieces recovered from Glass-glass panel after a process duration of 240s (left) and 720s (right). The EVA pieces appear cleaner with less silicon sticking to the surface after longer process duration.

418

419 **3.3 Analysis of metal content in the recycled c-Si PV panels**

420 It was necessary to ascertain the contents of the coarse and fine powder recovered after the
421 electrohydraulic fragmentation process to design the process to recycle metal and silicon. For
422 these analyses, powders recovered after processing the glass-glass and glass-backsheet panels
423 were used. Figure 8 shows the image of coarse and fine powder obtained after the
424 electrohydraulic treatment of the glass-glass panels under optical microscope. With the help of
425 optical microscope, the glass particles in the coarse powder could be easily identified. The
426 opaque particles could either be Si, Ag and Al from the solar cells. The fine powder also
427 contained glass particles along with silicon and metal particles, however, the proportion of
428 opaque silicon and metal particles were visibly higher than in the coarse powder. No visible
429 difference in the size and morphology of the particles could be observed in the powders
430 recovered from the treatment of the glass-glass and glass-backsheet panels.

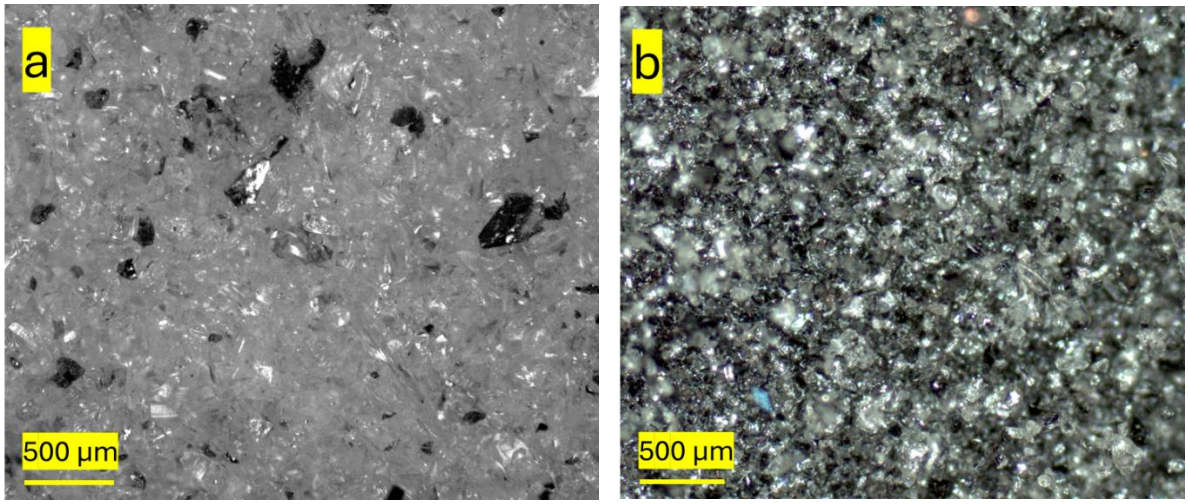

Figure 8: Optical microscopic image of the a) coarse and b) fine powder obtained after the electrohydraulic fragmentation of the glass-glass panels.

431

The powder was further analysed using Scanning electron Microscopy and the composition of the powder was ascertained using the Energy Dispersive X-ray spectroscopy (EDS). To analyse the powders, they were fixed on an adhesive and conductive carbon tape. Figure 9 shows the SEM images of the coarse and fine powders obtained after the treatment of the glass-glass panels at different magnifications. The carbon tape in the background could be seen in the coarse powder, however, the fine powder appears to cover the surface almost completely. From SEM images it can be seen that some particles in the coarse powder are smaller than 250 µm, which were retained with the larger particles during the manual sieving process.

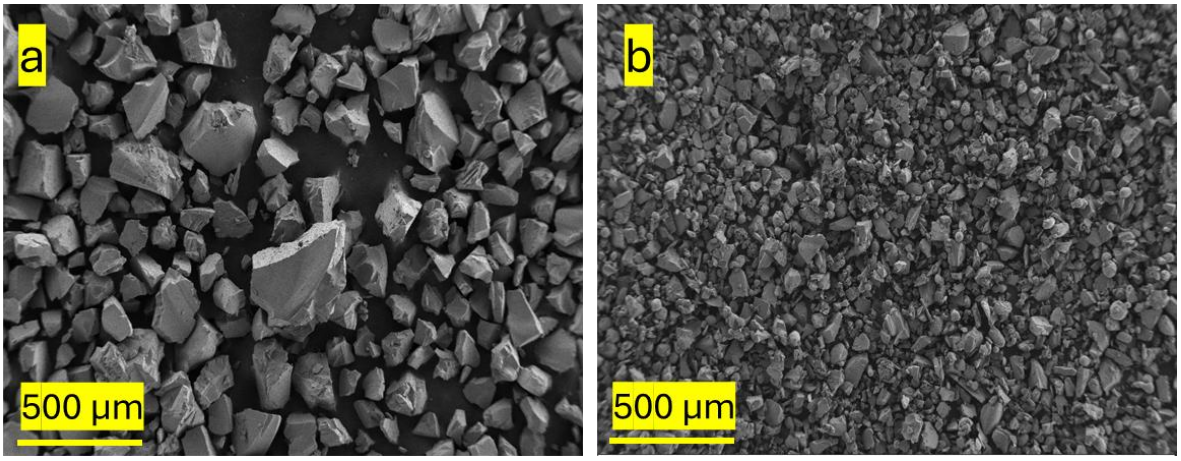

Figure 9: SEM images of the a) coarse and b) fine powder obtained after the electrohydraulic fragmentation of the glass-glass panels.

Figure10 and 11 show the EDS elemental maps of the coarse and fine powders respectively after processing the glass-glass panels. The coarse particles were mainly composed of glass particles as could be seen the EDS maps in Figure 10.

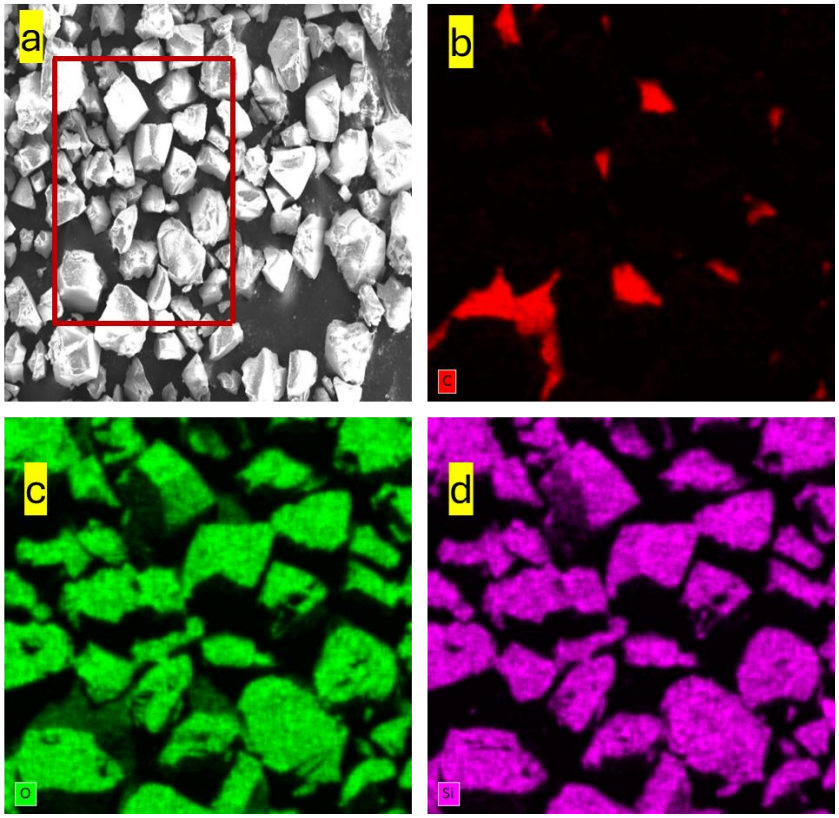

Figure 10: Elemental maps of coarse powder obtained by EDS showing a) the area of analysis b) carbon c) Oxygen d) Si

The glass made up 99% of the weight of the coarse particles according to the elemental analysis. Along with Si and Oxygen, small amounts of Ca, Na, and Mg were also found to be associated with the regions where both Si and O were present. These elements are usually added to glass during manufacturing of the glass meant to be used for fabricating PV panels [67].The carbon seen in the image corresponds to the carbon tape used for mounting the powder. The polymer pieces were effectively separated during the filtration process and were not found to be present in the coarse powder.

The presence of metal and Si pieces from the solar cells were confirmed in the fine powder by EDS analysis. As shown in figure 11-f, the brightly lit areas of Si correspond to the c-Si pieces from the solar cells, as oxygen is not prominent at those places in the corresponding oxygen map in figure 11-e. Al agglomerates were also confirmed to be present in the fine powder as shown in figure 11-c. The presence of Ag was difficult to ascertain due to the fine particle size and small amount. However, certain agglomerated particles of Ag were identified due to the strong signal associated with them. One such agglomerated Ag particle in highlighted within a circular region in figure 11-b. The observation agrees with the sizes of the Ag and Al particles used in the metal pastes for fabrication of solar cells [77–80]. The source of carbon in the map could be identified decisively. The spots of carbon appear to be bright in places where there was space between the particles. The pieces of polymers could not be decisively identified

using SEM; however, it is possible for the powder to include micro-sized or nano-sized polymer pieces.

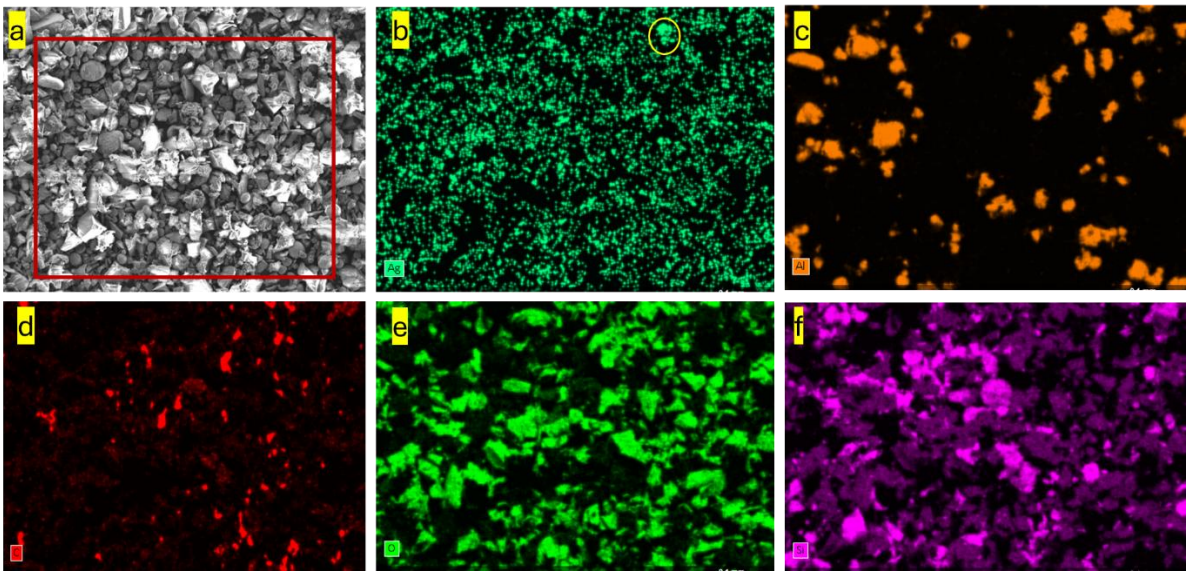

Figure 11: Elemental maps of fine powder obtained by EDS showing a) the area of analysis b) Ag c) Al d) Carbon e) Oxygen and f) Si. An agglomerated Ag particle is highlighted in (b).

Table 3 shows the %mass of the elements as determined by EDS measurements for the coarse and the fine powders. It can be clearly observed that the amount of Si and Al in the fine powder was much higher than the respective concentrations in the coarse powder. The percentage of Ag in the fine powder was determined in the range of 0.15-0.2% by mass using EDS, however the relative error associated with Ag was highest (≈ 20%). On the other hand, the relative errors associated with all other elements were within 2 - 4.5%.

Table 3: Mass% and atomic % of the elements in the coarse and fine powders obtained after the electrohydraulic treatment as detected using EDS technique.

Elements	Atomic number	Coarse powder		Fine Powder	
		Mass % [%]	Atomic % [%]	Mass % [%]	Atomic % [%]
Carbon (C)	6	10.8	18.4	3.5	6.7
Oxygen (O)	8	42.4	51.7	22.9	32.8
Aluminium (Al)	13	0.5	0.3	13.4	11.3
Silicon (Si)	14	37.1	25.8	53.7	43.8
Silver (Ag)	47	-	-	0.17	0.04

Finally, to accurately assess the content of Ag in the powder, the powder was analysed using inductively coupled plasma optical emission spectroscopy (ICP-OES) method. The results from the measurements are shown in Table 4. The solution with the coarse powders and fine powders had dilution factors of 1 and 10 respectively.

Table 4: ICP-OES analysis of coarse and fine powder recovered from GG, GB and GF PV panels after electrohydraulic fragmentation process.

Powder type (Dil.)	ppm Ag	Ag [mg]	Ag [%]
GB coarse (X1)	41.03	3.41	0.02
GB fine (X10)	4.86	4.03	0.15
GG coarse (X1)	42.01	3.49	0.02
GG fine (X10)	7.03	5.84	0.20
GF coarse (X1)	18.1	1.5	0.01
GF fine (X10)	3.15	2.6	0.13

From the OES measurements, the presence of Ag particles in the fine powder could be confirmed. The concentration of Ag in the fine powders from all the three types of panels were found to be in the range of 0.15-0.2% wt. The results from the OES measurements agreed with those of the EDS measurements, despite the higher measurement error recorded during the latter.

3.4 Separation and recovery of metals and Si.

As mentioned earlier, Ag is the one of the most valuable components that can be obtained from a PV panels, despite being present in quantities less than 0.1% wt. High quality Si have been obtained only using thermal delamination or decomposition processes [38,48,81,82]. In this work, efforts were made to separate Ag, Al and Si, while maintaining their individual recoverability. The fine powder obtained from electrohydraulic treatment of GG and GB panels were mixed in the ratio 1:1 and were used for subsequent recovery experiments. As seen earlier, the fine powder contains glass powder, silicon and metals such as Ag and Al. A portion of the fine powder (without any further chemical treatment) was melted in an induction furnace under Argon atmosphere to obtain a silicon ingot. Later the cross section of the sample was prepared and analysed under SEM. Figure 12 shows the SEM image and the EDS maps of the sample. The metal appears as bright region in the dark Si matrix. This was further confirmed by EDS mapping as shown in Figure 12. The Ag and Al were found to be present in the same areas both inside the crystals and along the grain boundaries and their elemental maps were overlapped. These were probably Ag-Al eutectic formed during the solidification process after melting [83–86]. The fraction of individual components in terms of % wt. of Si, Al and Ag was estimated to be 96 ±1%, 1.2±0.2 % and 0.2±0.1% respectively from the EDS measurements.

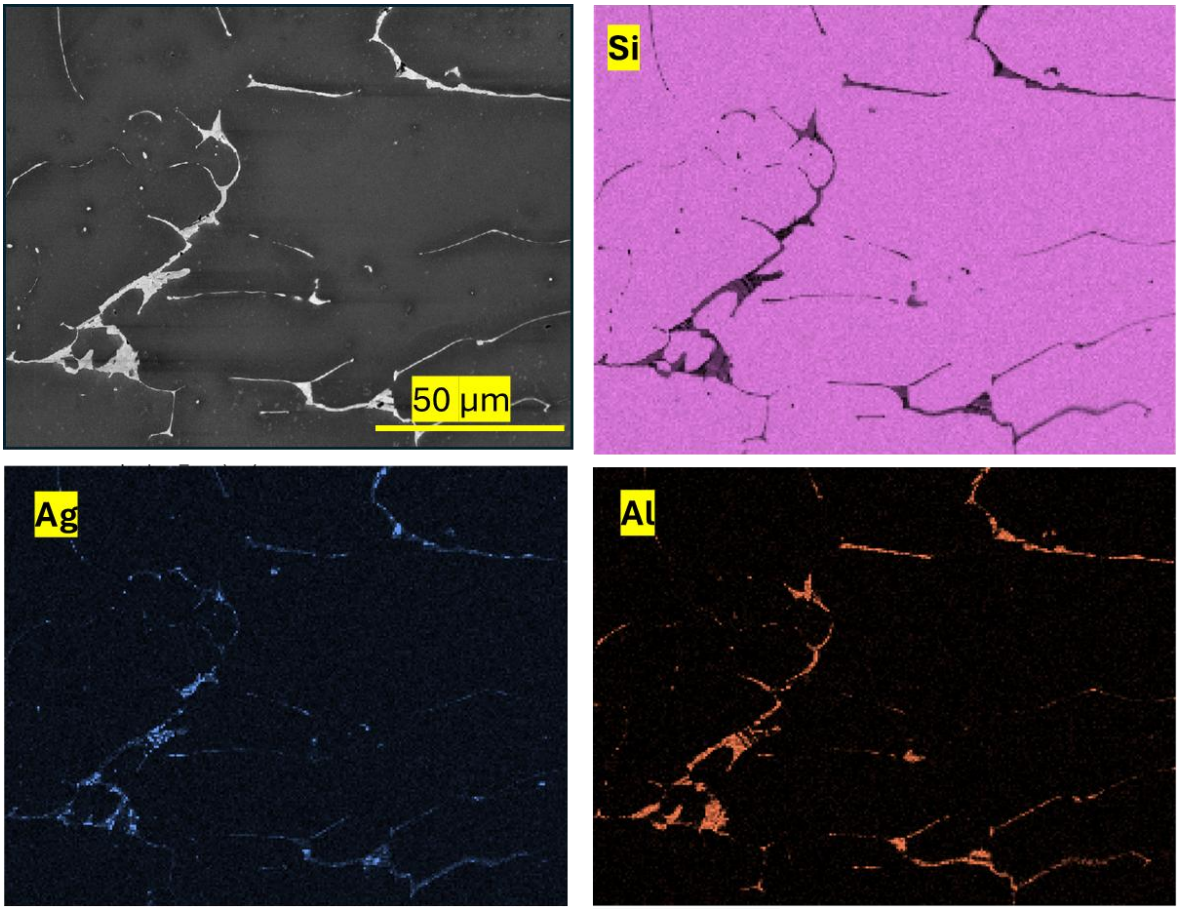

Figure 12 – SEM image and EDS elemental maps of the sample prepared by melting the fine powder after the treatment with HF.

While HF can be used to dissolve glass, the acid will also react with Al and Ag. The possible reactions of HF with SiO_2 Ag and Al are given in equations 1-3.

$$SiO_2 + 4HF \rightarrow SiF_4 + 2H_2O \quad \text{(eq-1)}$$

$$2Al + 6HF \rightarrow 2AlF_3 + 3H_2 \quad \text{(eq-2)}$$

$$2Ag + 2HF \rightarrow 2AgF + H_2 \quad \text{(eq-3)}$$

The SiF_4 is gas at room temperature and effuses out. The SiF_4 gas is of commercial importance and has multiple uses in the semiconductor and chemical industries [87–90]. Using this process, the gas can be recovered at this point and stored for future uses [91]. Hydrogen also is a commercially important gas and if extracted can add to the economic viability of the process. To ensure a clean process which avoids mixing of commercially useful gases, and enhance the maximum resource utilization, it was decided to leach out Al first using sodium hydroxide (NaOH) solution. NaOH does not react with glass and Si, while with Ag it can form Ag_2O, AgOH and AgO, all of which are solid precipitates and are not readily soluble in water [92–94]. Hence, they can be retained in the solid form after filtration. The expected reaction between Al and NaOH is shown in equation-4 [95].

$$2Al + 6H_2O + 2NaOH \rightarrow 2NaAl(OH)_4 + 3H_2 \quad \text{(eq-4)}$$

The $NaAl(OH)_4$ is soluble in water and can be separated from the remaining solid powder using filtration. Ag is expected to form oxides which are insoluble in NaOH and precipitate, while Si does not react appreciably with NaOH at room temperature. This reaction also releases H_2 which is a commercially important gas that can be extracted and stored. The process of creating hydrogen using Al and NaOH have been suggested as viable routes for production of hydrogen [95–97]. Furthermore, the exhausted NaOH could easily be regenerated from $NaAl(OH)_4$ formed during the reaction and the $NaAl(OH)_4$ could itself be used in paper production industry and water treatment plants among other commercially important uses [96,97]. However, collection and storage of H_2 was not attempted in this work. Another advantage of using NaOH solution for leaching Al is that it can dissolve any remaining Al embedded into Si during the process of contact formation [98].

Leaching of Al was carried out using sodium hydroxide (NaOH) solution (1M) at 60 ℃ for 10 minutes. The powder was taken in a beaker and sufficient quantity of 1M NaOH solution was added to it. The beaker was left undisturbed on a heater set at 60 ℃ for 10 minutes, which was found to be sufficient to dissolve the Al in the powder. The powder was again filtered, washed and dried in a hot air oven at 120C for 30 min. A portion of the NaOH treated powder was melted in the furnace and the sample was analysed with SEM. Figure 13 shows the SEM image and the EDS map of the Si samples obtained after treatment with NaOH. While Ag could be observed in the EDS map, Al was not detected.

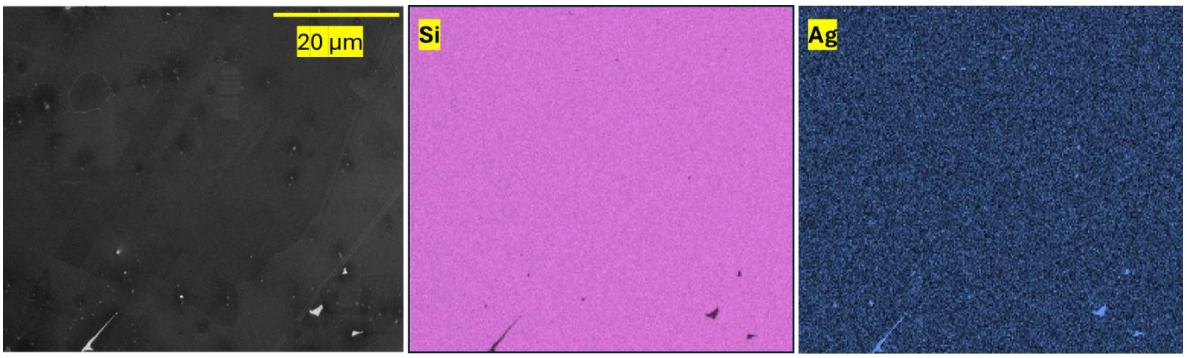

Figure 13 – SEM images of the sample prepared by melting the fine powder obtained after the treatment with HF and subsequent treatment with NaOH.

The recovery of Ag from the powder was done using HNO_3 solution which is commonly suggested in literature [10,99,100]. The Ag in the powder is expected to form AgO on reaction with NaOH [92–94]. The probable reaction between AgO and HNO3 is presented in equation. 5.

$$AgO + 2HNO_3 \rightarrow Ag(NO_3)_2 + H_2O \quad \text{(eq-5)}$$

The $AgNO_3$ is soluble in the aqueous HNO_3 and hence can be easily extracted by simple filtration process. In this work, we used commercially available 49% nitric acid solution, and the process was carried out at 70℃ for 10 minutes. Later the solution was cooled and filtered. Upon analysis using ICP-OES, the solution was found to contain between 3-7 ppm of silver, which agrees with the value initially assessed without any chemical treatment of the powders.

While recovery of high-quality silver is not attempted in this work, separation of silver from silicon in a form, from which pure Ag can be recovered later, was achieved successfully.

During treatment of the powders with HNO_3, silicon is expected to be oxidized and covered in an ultrathin later of SiO_x .This process has been used to create oxide films on bulk silicon [101,102], and the thickness of the oxide is shown to be dependent on the temperature of the acid [103,104]. At 50°C, the thickness of the oxide is expected to be rather thin in the range of 1-2nm. After the treatment with nitric acid, the remaining powder is primarily composed of glass and silicon particles. At this stage the silicon particles originating from the solar cells are also expected to include the ARC layer. In order to remove glass powder and the ARC layer from the silicon particles originating from the solar cells, the samples were treated with dilute HF (5% wt.). HF reacts with glass but does not appreciably consume Si, providing a good selectivity. The HF reacts with glass (SiO_2) and produces SiF_4, and H_2O as shown in equation-1. The HNO_3 treated powder (after drying) was taken in a beaker and sufficient quantity of HF (at room temperature) was added slowly to the powder. The HF+powder beaker was left to stand for an hour, after which the powder was filtered using a filter paper, washed thoroughly with DI water and dried in an oven. For initial mass of 10g, ≈3-4 g powder was obtained after treatment with HF. Hence, from this experiment it could be concluded that the fine powder was composed of ≈50-60% glass particles. After the reaction of glass with HF, the remaining powder is expected to contain only Si. The powder obtained after HF treatment was washed with DI water, dried in an oven. The powder was melted in the furnace (≈1550-1600 °C), solidified and analysed using SEM. Figure 14 shows the SEM image and the EDS map of the treated silicon sample. The sample was confirmed to be primarily Si with no detection of Al and Ag. Further confirmatory tests were conducted using ICP-OES to analyse the treated Si powder, which could not detect Ag and Al in ppm levels in five measurements. However, at this stage, Pb and Cd were detected (≈10-25 ppm), as no efforts were made to specifically remove them from the Si. To understand the efficacy of the process designed in this work in removing Ag and Al from Si, the samples were further analysed using ICPMS, where Ag and Al were found to be present, their values ranging between 4-14 ppb. Therefore, at this point the silicon is not ready for reinjection into the value chain. Nevertheless, the process demonstrates capability of removing Ag and Al from the silicon powder obtained after EHF processing. The quality of the silicon could be further improved upon optimization in the process parameters and designing processes to remove other metals associated with the recycled Si. This agrees with the published results where researchers have recovered high silicon from thermally recycled panels using prolonged chemical treatments [40,41].

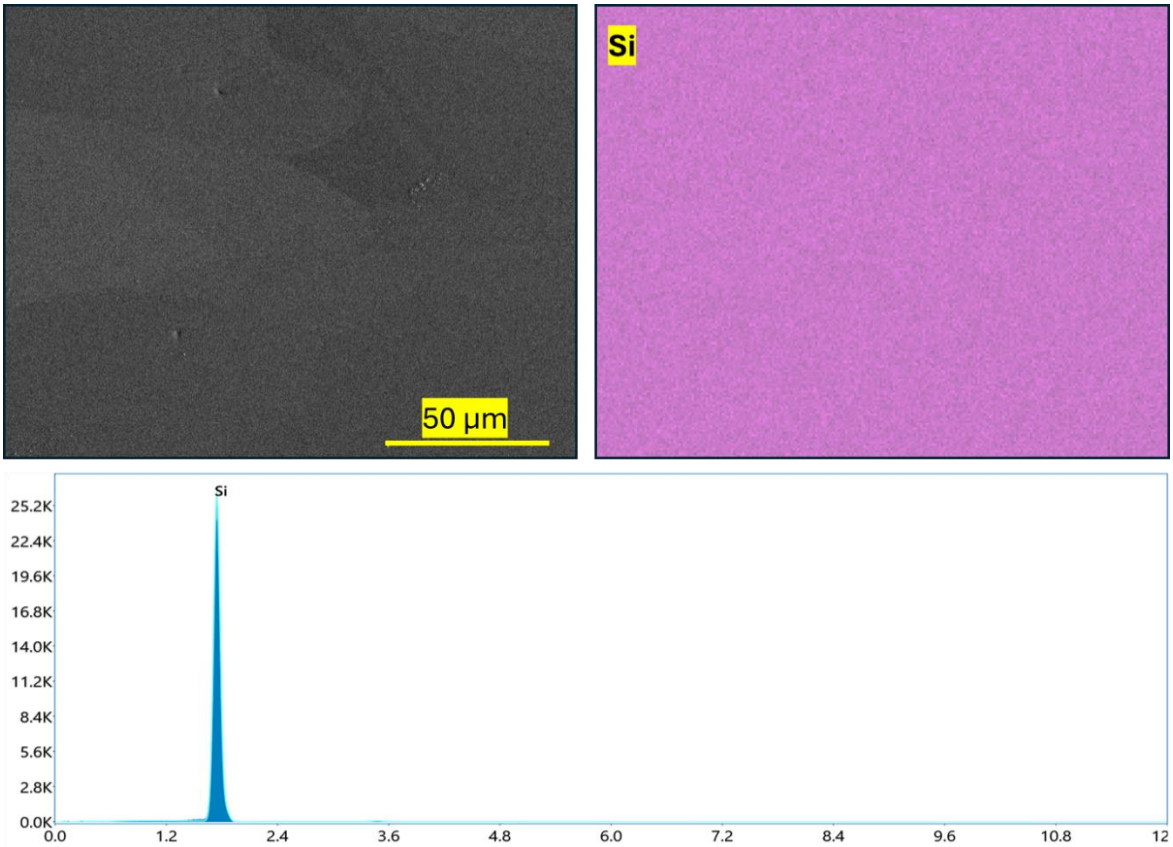

Figure 14 – SEM and EDS of the Si powder obtained after the chemical treatment. The EDS plot showing the clear signal in Si.

3.5 Separation and recovery of polymers

In most of the recycling processes, the polymer is pyrolyzed at high temperature as its recovery is not considered either technologically feasible or economically viable [7,20,105–107]. One of the advantages of the electrohydraulic processing of PV panels is the complete delamination of the polymer layers from the glass and solar cells. As explained earlier, depending on the type of panel the polymers recovered can be either EVA layers (glass-glass panels) or a combination of EVA and front/rear layers in the case of glass-backsheet or glass free panels. The recovery of the polymers was attempted using the chemical route. The recovery of the polymers is expected to be the easiest for the glass-glass panels due to the presence of only EVA as the encapsulant and the removal of almost all the silicon during the electrohydraulic fragmentation process. The polymer pieces recovered from different types of panels are shown in figure 15. It was observed that the EVA polymers recovered from the glass-glass panels were the cleanest and had least amount of silicon particles sticking to them. The polymer pieces recovered from the glass free panels had the maximum amount of silicon sticking to the surface. While longer process times was effective in removing silicon particles sticking to the polymer surface in the glass-glass and glass-backsheet panel, the impact was not visibly apparent for the glass-free panels. Furthermore, the EVA pieces from the glass-backsheet panels has less silicon particles sticking to them that those to the EVA+PET pieces from the same panel, as can be seen in figure 15.

The exact composition of the EVA films differs slightly depending on the producer and the brand, however, the EVA used in the PV industry as encapsulant contains several additives such as UV absorber, photo antioxidants and thermo-antioxidants in addition to the vinyl acetate copolymer [108–111]. Hence, we first tried dissolving non-heat-treated polymers, to understand the effect of organic solvents on the particular polymer films being used in this work. To test the solubility of the polymers in chemicals, the raw samples from the EVA and the backsheet layers were used without any heat treatment. EVA is known to dissolve in chloroform, toluene, acetone and other organic solvents [112–115]. Pieces of unprocessed EVA (≈ 10 g) were first dissolved in 100 ml of $CHCl_3$ at 50°C. The EVA was completely dissolved within 180s. Since, both the white backsheet and the transparent front sheet are made of PET based polymers, they were experimented together for solubility. 10g of untreated backsheet (white) and front sheet (transparent) were added to a solution of NaOH+ Ethylene Glycol (E.G) (10g NaOH in 100 ml E.G.) and was heated to 150°C. The solution was stirred manually with the help of a quartz stirrer. Both PETs were almost completely dissolved in the solution at t=120 min. Only 5% of the original mass of the polymer from the white rear backsheet was undissolved. Glycolysis of PET is a common commercial method of recycling PET and is carried out at higher temperature and pressure, often in the presence of a catalyst [12,13,116]. However, carrying out such processes require special chambers that were beyond the scope of this work and hence the focus of this work was limited to the successful cleaning of the recovered polymer pieces and separating the EVA from the PET backsheet/front sheet.

Figure 15 – Pieces of polymer recovered from the different panel types after the electrohydraulic treatment.

The solubility of the heat-treated EVA pieces obtained from the glass-glass and glass-backsheet panels were determined first. The polymers pieces obtained after the electrohydraulic treatment were cleaned of the silicon particles sticking to the surface by dipping them into a solution of concentrated KOH (20%) maintained at 70°C for 10 minutes. This is a common process used for etching silicon in the production of solar cells [117]. After KOH etching the polymer pieces were washed in DI water. However, the pieces could not be dissolved completely in chloroform at elevated temperatures (50-60 °C) despite keeping the pieces for more ≈ 96 hours under magnetic stirring. Toluene was found more effective in dissolving heat-treated EVA. The EVA pieces appeared to be softer in appearance after ≈ 96 hours of dissolving in toluene at 80°C using magnetic stirring, but still they were not completely dissolved.

To separate the pieces of EVA+PET obtained from the glass-backsheet and glass-free panels, the joined pieces were kept in different solutions at different temperatures and for different durations. After the experiment, the number of pieces separated completely were calculated manually and expressed as a percentage of the number of pieces used for the particular experiment. The details of the experiment are listed in table 5.

Table 5: Results of chemical treatment to separate the EVA+PET pieces obtained from the glass-backsheet panels, after cleaning them in KOH. The percentages are rounded off to the nearest whole number.

	Chem-1	T [°C]	t [hours]	Chem- 2	T [°C]	t [hours]	Delamination
1	Chloroform	50	96	-	-	-	No
2	Toluene	90	96	-	-	-	Partial
3	-	-	-	NaOH+ E.G	150	2	Yes (≈55%)
3	Chloroform	50	24	NaOH+ E.G	150	2	Yes (≈75%)
4	Toluene	80	24	NaOH+ E.G	150	2	Yes (≈ 99%)

Soaking the pieces only in chloroform and toluene were not sufficient to delaminate the EVA and PET layers. When the pieces were soaked in Toluene at 90°C for 96 hours, with continuous magnetic stirring, partial delamination could be observed. However, complete delamination of the EVA+PET layers could not be achieved for any of the pieces. The pieces were then kept in a solution of NaOH+E.G solution as used earlier at 150°C for 120 minutes. In this case, delamination was achieved for approximately half of the samples. Then a two-step process was designed whereby the pieces were first dipped in either chloroform and toluene followed by the E.G and NaOH solution. When the pieces were first dipped in chloroform at 50°C for 24 hours, followed by E.G+NaOH solution at 150°C for 2 hours, ≈75% of the pieces were completely delaminated. Of the remaining pieces, some were partially delaminated while ≈ 10% of the pieces showed swelling but no delamination. Soaking the pieces in toluene at 90°C for 24 hours followed by soaking them in the E.G+NaOH solution at 150°C for 2 hours was most effective and resulted in 99% separation of the EVA from the PET sheet. All samples were either partially or completely delaminated. Furthermore, the partially delaminated samples were easily separated manually. Hence, we surmise a commercial process with violent agitation could be more effective is separating the EVA from the backsheet layers and achieve complete delamination quicker. However, it should be noted that complete dissolution of the heat-treated polymers in any of the solution was not obtained. The aim of this work was only to achieve cleaning and delamination of polymer pieces stuck together so that they could be further processed under specific conditions for recycling.

3.6 Impact of the age of the modules on the recycling process

A key aspect of this work which differentiates it from the actual application in a commercial setting is the age of the panels. In this work, the modules were fabricated in the laboratory, because it was difficult to obtain old modules, specifically of different types (GG, GB and GL). Further, having similar polymeric materials and similar fabrication processes simplified the

analysis of the results obtained. While this approach could be justified for controlled experiments in the laboratory, in real world, the modules may have aged differently, under different conditions and may have different materials. To test the impact of ageing on the modules, old GB modules fabricated in our laboratory, with age ranging between 5-10 years were processed according to the experimental design presented in this work. Some of these modules had been exposed to solar irradiation and had been in active operation (in our rooftop test bed), some were used for accelerated degradation testing and then stored while some were simply stored in a container inside the building in an uncontrolled environment. We shall refer all these modules as 'old modules'. The processing parameters were kept similar for all the modules. The overall yield and physical properties of Si and glass powder obtained after EHF processing of the old modules were similar to the results obtained earlier with the newly fabricated modules. However, visible difference was observed with respect to the polymer separation. Almost all of the polymers (EVA+PET) pieces from the old modules were partially separated (to varying degrees) in the EHF process step itself. When the experiment was conducted with relatively newer modules, the separation was observed only for a few samples. This is not unexpected as the backsheet degradation is the most observed failure mode in the modules [118–120]. However, the amount of delamination could not be quantified, and no visible trend was observed in the delamination of the samples with the age of the modules. For example, in one experiment, the polymer pieces from the oldest module exposed to solar irradiation showed more delamination than those from the modules of similar age that have been subjected to degradation tests and stored. While the reasons behind such observations could not be determined in this work, it could be related to the defects in the modules during fabrication, or to the difference in the ageing behaviour of the modules with and without solar irradiation [118,121]. More focussed efforts and a careful experimental design would be required to understand the ageing of modules and their response to the recycling treatment. However, across the aged modules, the polymer layers took less time to be delaminated using the Toluene and NaOH+E.G solution, than in the case of the relatively newer modules. In some instances, complete delamination was obtained in less than 60 minutes of NaOH+E.G treatment. However, no reproducible trend could be observed with the age or exposure of the modules and the time taken for complete delamination. While complete delamination was achieved in less than 100 minutes for all the samples tested, the samples from the oldest modules or the modules exposed to solar irradiation for the longest duration were not always delaminated in the shortest duration. Several factors could be responsible for these observation as it has been known that both extrinsic (climatic conditions, temperature and humidity cycles) and intrinsic (materials, manufacturing process and internal stresses) factors can contribute to degradation of polymers [121–125]. This highlights the difficulty in conducting experiments with uncontrolled samples. Further research is necessary to correlate the ageing in the polymers to the response to the EHF and further recycling processes. Nevertheless, this experiment shows that the EHF process can be applied not only to different types of modules, but also to modules with different age and exposures. This further supports the suitability of the EHF process to the real-world applications in PV recycling.

3.7 Possible pathways of recycling materials obtained after EHF processing.

In this work, we have used the EHF process to extract and separate the different materials used in the fabricating of the solar PV modules. The process involving complete recycling the materials and obtaining them in a commercially usable form is beyond the scope of this work. However, to establish the usefulness of the EHF process, we try to provide a feasible pathway to utilize the materials obtained after EHF processing of EOL Si PV modules.

Polysilicon is mostly produced using Siemen's process or in some cases, using a fluidized bed reactor [126–129]. In Siemen's process, the end product is in the form of rods or ingots which are further processed into monocrystalline using Cz process [130]. Using bed reactor process, the silicon obtained is usually granular, which is later melted to make poly-Si or Cz-Si. In this work, we obtained Si powder, which was melted in induction furnace to make Si ingots. We believe this technology is the easiest to implement and scale up for commercial applications. Both Arc and induction furnaces could be used for melting silicon [131,132]. In addition, the contaminated portion of Si ingot which cannot be reintroduced into polysilicon production process and is usually discarded, could be used for other metallurgical processes such as for production of ferrosilicon and metallurgical grade Si, which are still commercially valuable materials [133,134]. While fine Si powder could raise some issues with material handling, this could be solved using proper material handling equipment. Hence, once the metallic, glass and other impurities are removed from Si, it can be easily melted and cast into ingots for further use [36,135,136].

Ag can be obtained in granular form from the dissolved state in HNO_3 solution. For recovery of silver, HNO_3 leaching followed by precipitation or electrolysis have been proven to be effective processes [10,98–100,137]. Using chemical pathway, after leaching, the $AgNO_3$ in the HNO_3 solution can be reduced using agents like aluminium, copper, iron, zinc, formaldehyde, chloride salts or sodium carbonate (or combinations of more than one of these) to precipitate Ag. The Ag precipitate can be washed and dried to give silver powder [137–142], which can directly be used in manufacturing new Ag metal pastes [143,144].

Recycling glass obtained after the EHF processing of the EOL PV modules is not expected to be a complicated process. The large glass pieces and the coarse glass powder can be washed which would remove any Si/metal powder sticking to its surface, along with any stray pieces of polymer. After washing the glass can be sent for recycling and can be made into new glass sheet for use in the fabrication of new PV modules [145–148].

Recycling of the polymers obtained from the EOL PV modules appears to be the most difficult part of recycling. Dissolving EVA and PET in organic solvents usually requires high temperature, pressure and longer treatment durations, all of which could result in higher recycling costs. The polymers dissolved in the solution could be recovered by spreading the solution over a temperature-controlled surface and allowing the organic solvent to evaporate. In our laboratory setting, we were successful in obtaining a thin layer of EVA after dissolving it in toluene for extended period of time and spin coating the dissolved solution. The rate of dissolution could be increased under higher pressure and temperature [12,13,149]. While such layers of EVA and PET could be obtained using glycolysis followed by flat die extrusion, their

reusability in the PV modules and the subsequent impact on the reliability of the modules needs to be evaluated.

4. Conclusion

With increase in the deployment of PV systems globally, efficient handling of the EOL PV panels is a crucial step to further enhance the sustainability of PV panels. Development of processes enabling complete recycling of silicon PV panels is essential to improve the circularity of silicon PV panels. In this work we have presented a step-by-step process of recycling the end-of-life c-Si PV panel using electrohydraulic fragmentation process. While electrohydraulic fragmentation process has been studied earlier as an effective separation process, in this work we have developed a step-by-step process to recover high quality raw materials from the yield of the electrohydraulic fragmentation process. The electrohydraulic process helps in achieving high quality separation of the ribbons, glass, silicon along with metal and the polymers. The process effectively separates the silicon from the polymer pieces, while recovering the polymer pieces as well. Since the process is carried out at room temperature and the polymer layers are not burned off, this process could be more environmentally friendly, producing lower exhaust. Furthermore, this process has among the highest yield as more than ≈99.5% of the weight of the panel is recovered. The process needs just electrical energy as input which could be generated using environment-friendly energy sources, technically making it possible for the process to have a lower carbon footprint than the thermal delamination process.

The impact of the different process parameters such as the type of panel, feed size and pulse duration were studied in this work. It was observed that the glass-glass panels were the easiest to delaminate. The delamination process was most effective for a given size of the feed material for glass-glass or bifacial panels. This was due to the basic operating principle of the electrohydraulic delamination process which relies on the difference in the mechanical properties of materials to achieve efficient delamination. Hence, it can be said that bifacial panels, while producing higher energy during their lifetime [150–154] , and are finding new areas of applications such as agrophotovoltaics [155,156] and building integrated photovoltaics [157,158] are also better suited for recycling processes, as they have lower polymer content. It was shown in this work, that in addition to ease in processability using electrohydraulic treatment, the recovered materials, especially polymers were cleaner and had less silicon sticking to them. Conversely, this implies more silicon could be recovered from glass-glass panels. The glass-free panels could be delaminated only when they are cut into smaller pieces (2.5 x 2.5 cm^2). The products recovered were sorted by size. The glass was mostly obtained as small pieces (1-5 mm) and coarse powder (>250 μm). Silicon and metal were mostly obtained as fine powder (<250 μm). The recovery of Al, Ag and Si was done using chemical methods. Another advantage of the electrohydraulic fragmentation process is the recovery of fine powder (< 250 μm). The fine, small size of the particles enable quick chemical reactions due to the enhanced surface area and hence could improve the process throughput in industrial applications. A step-by-step process flow was designed to recover Al, Ag and Si from the fine powder recycled panels. Table 6 shows the summary of materials recovered and the by-products created during the process.

Table 6: Summary of the different process used, and the materials recovered in this work.			
Sr. no	Material recovered	Process used	By-products/comments
1	Al Frame	Mechanical removal	Before electrohydraulic fragmentation
2	Plastic junction box	Mechanical removal	Before electrohydraulic fragmentation
3	External Copper wires	Mechanical removal	Before electrohydraulic fragmentation
4	Copper ribbons	Electrohydraulic fragmentation	None
5	Glass pieces (big pieces and coarse powder)	Electrohydraulic fragmentation	Bits of silicon, metal and plastic
6	Fine powder (Glass, Si and metal)	Electrohydraulic fragmentation	None
6.1	Al	Treating fine powder with NaOH	H_2
6.2	Ag	Treating fine powder (after NaOH) with HNO_3	H_2O
6.3	Si	Treating fine powder (after NaOH and HNO_3 treatment) with HF	$SiF_4 + H_2O$
7	Polymers (separation of EVA from PET)	Treating with KOH (for removing Si), Toluene and NaOH+E.G solution.	Cleaned polymer layers separated for further recycling.

The process flow suggested in this work can be easily adopted in the industry leading to complete recycling of the c-Si PV panels. The separation of different sizes of powders could be achieved by employing a graded filter. The powders can be dried using an inline drier and later processed accordingly. Recycling of the polymers used in the PV modules still remains a challenge and needs further attention and research. Nevertheless, in this work we have shown that recycling end-of-life PV panels using electrohydraulic fragmentation can lead to a high yield and high quality of materials enabling almost complete recyclability of silicon PV panels. Future work would comprise of installing a pilot line and establishing the industrial process for recycling end-of-life c-Si PV panels using electrohydraulic delamination process. Furthermore, as pointed out earlier, the impact of the ageing of the modules under different conditions (such as stored vs irradiated, active in different climate zones, different age of the modules) should be investigated to analyse the suitability, and aid in optimization of the EHF process for commercial recycling activities.

Acknowledgement

A part of this research is supported by the Solar Energy Research Institute of Singapore (SERIS) at the National University of Singapore (NUS). SERIS is supported by the National University of Singapore (NUS), the National Research Foundation (NRF), the Energy Market

Authority of Singapore (EMA) and the Singapore Economic Development Board (EDB).The work was also supported by National Research Foundation, Singapore, Ministry of National Development and the National Environment Agency, under the Urban Solutions and Sustainability Integration Fund (USS-IF-2019-5).

Some elements of this research are also a part of the project No. 2022/45/P/ST5/02712, executed at AGH University of Krakow, co-funded by the National Science Centre, Poland and the European Union Framework Programme for Research and Innovation Horizon 2020 under the Marie Skłodowska-Curie grant agreement No. 945339.

References

[1] IRENA (2019), Future of Solar Photovoltaic: Deployment, investment, technology, grid integration and socio-economic aspects, Abu Dhabi, 2019. https://www.irena.org/publications/2019/Nov/Future-of-Solar-Photovoltaic (accessed September 8, 2023).

[2] Gaëtan Masson, IEA - 2024 Snapshot report of Global PV Markets, 2024. https://doi.org/10.69766/VHRF4040.

[3] G.M.A. 'Detollenaere, I. 'Kaizuka, A.J. 'Waldau, J. 'Donoso, IEA-PVPS Snapshot of Global PV Markets 2021, 2021. https://iea-pvps.org/snapshot-reports/snapshot-2021/ (accessed September 8, 2023).

[4] S. Weckend, A. Wade, G. Heath, End-of-Life Management: Solar Photovoltaic Panels, 2016. https://www.irena.org/publications/2016/Jun/End-of-life-management-Solar-Photovoltaic-Panels (accessed September 8, 2023).

[5] F. Ise, P. Projects GmbH, Photovoltaics Report-Fraunhofer Institute for Solar Energy Systems, ISE with the support of PSE Projects GmbH, 2024. www.ise.fraunhofer.de.

[6] P.H. Chen, W.S. Chen, C.H. Lee, J.Y. Wu, Comprehensive Review of Crystalline Silicon Solar Panel Recycling: From Historical Context to Advanced Techniques, Sustainability (Switzerland) 16 (2024). https://doi.org/10.3390/su16010060.

[7] K. Komoto, J.-S. Lee, J. Zhang, D. Ravikumar, P. Sinha, A. Wade, G.A. Heath, End-of-life management of photovoltaic panels: trends in PV module recycling technologies, National Renewable Energy Laboratory (NREL), Golden, CO (United States), 2018. https://doi.org/https://doi.org/10.2172/1561523.

[8] A. Mulazzani, P. Eleftheriadis, S. Leva, Recycling c-Si PV Modules: A Review, a Proposed Energy Model and a Manufacturing Comparison †, Energies (Basel) 15 (2022). https://doi.org/10.3390/en15228419.

[9] A. Divya, T. Adish, P. Kaustubh, P.S. Zade, Review on recycling of solar modules/panels, Solar Energy Materials and Solar Cells 253 (2023) 112151. https://doi.org/https://doi.org/10.1016/j.solmat.2022.112151.

[10] R. Deng, Y. Zhuo, Y. Shen, Recent progress in silicon photovoltaic module recycling processes, Resour Conserv Recycl 187 (2022) 106612. https://doi.org/10.1016/j.resconrec.2022.106612.

[11] R. Einhaus, F. Madon, J. Degoulange, K. Wambach, J. Denafas, F.R. Lorenzo, S.C. Abalde, T.D. García, A. Bollar, Recycling and Reuse potential of NICE PV-Modules, in: 2018 IEEE 7th World Conference on Photovoltaic Energy Conversion (WCPEC)(A Joint Conference of 45th IEEE PVSC, 28th PVSEC & 34th EU PVSEC), IEEE, 2018: pp. 561–564. https://doi.org/10.1109/PVSC.2018.8548307.

[12] V. Sinha, M.R. Patel, J. V Patel, PET waste management by chemical recycling: a review, J Polym Environ 18 (2010) 8–25. https://doi.org/10.1007/s10924-008-0106-7.

[13] D.S. Achilias, G.P. Karayannidis, The chemical recycling of PET in the framework of sustainable development, Water, Air and Soil Pollution: Focus 4 (2004) 385–396. https://doi.org/10.1023/B:WAFO.0000044812.47185.0f.

[14] R. Deng, Y. Zhuo, Y. Shen, Recent progress in silicon photovoltaic module recycling processes, Resour Conserv Recycl 187 (2022) 106612. https://doi.org/https://doi.org/10.1016/j.resconrec.2022.106612.

[15] M.M. Lunardi, J.P. Alvarez-Gaitan, J.I. Bilbao, R. Corkish, A review of recycling processes for photovoltaic modules, Solar Panels and Photovoltaic Materials 30 (2018). https://doi.org/10.5772/INTECHOPEN.74390.

[16] R. Sanathi, S. Banerjee, S. Bhowmik, A technical review of crystalline silicon photovoltaic module recycling, Solar Energy 281 (2024). https://doi.org/10.1016/j.solener.2024.112869.

[17] J. Cui, L. Zhang, Metallurgical recovery of metals from electronic waste: A review, J Hazard Mater 158 (2008) 228–256. https://doi.org/10.1016/j.jhazmat.2008.02.001.

[18] R. Nithya, C. Sivasankari, A. Thirunavukkarasu, Electronic waste generation, regulation and metal recovery: a review, Environ Chem Lett 19 (2021) 1347–1368. https://doi.org/10.1007/s10311-020-01111-9.

[19] K. Klejnowska, W. Mijal, J. Golebiewska-Kurzawska, J. Strzelczuk, Recycling of end-of-life PV panels-a review of technologies, in: E3S Web of

Conferences, EDP Sciences, 2024. https://doi.org/10.1051/e3sconf/202455001040.

[20] X. Wang, X. Tian, X. Chen, L. Ren, C. Geng, A review of end-of-life crystalline silicon solar photovoltaic panel recycling technology, Solar Energy Materials and Solar Cells 248 (2022) 111976. https://doi.org/10.1016/j.solmat.2022.111976.

[21] J.A. Tsanakas, A. van der Heide, T. Radavičius, J. Denafas, E. Lemaire, K. Wang, J. Poortmans, E. Voroshazi, Towards a circular supply chain for PV modules: Review of today's challenges in PV recycling, refurbishment and re-certification, Progress in Photovoltaics: Research and Applications 28 (2020) 454–464. https://doi.org/10.1002/pip.3193.

[22] P.R. Dias, L. Schmidt, N.L. Chang, M.M. Lunardi, R. Deng, B. Trigger, L.B. Gomes, R. Egan, H. Veit, High yield, low cost, environmentally friendly process to recycle silicon solar panels: Technical, economic and environmental feasibility assessment, Renewable and Sustainable Energy Reviews 169 (2022) 112900. https://doi.org/10.1016/j.rser.2022.112900.

[23] D. Sica, O. Malandrino, S. Supino, M. Testa, M.C. Lucchetti, Management of end-of-life photovoltaic panels as a step towards a circular economy, Renewable and Sustainable Energy Reviews 82 (2018) 2934–2945. https://doi.org/10.1016/j.rser.2017.10.039.

[24] F. Cucchiella, P. Rosa, End-of-Life of used photovoltaic modules: A financial analysis, Renewable and Sustainable Energy Reviews 47 (2015) 552–561. https://doi.org/https://doi.org/10.1016/j.rser.2015.03.076.

[25] IEA-PVPS Report Number: T12-06:2016, IEAPVPS Report on End-of-Life Solar PV Panels, 2016. https://www.irena.org/-/media/Files/IRENA/Agency/Publication/2016/IRENA_IEAPVPS_End-of-Life_Solar_PV_Panels_2016.pdf (accessed February 4, 2025).

[26] The Silver Institute, Metal Focus, World Silver Survey, 2023. https://www.silverinstitute.org/wp-content/uploads/2023/04/World-Silver-Survey-2023.pdf (accessed February 4, 2025).

[27] R. Deng, Y. Zhuo, Y. Shen, Recent progress in silicon photovoltaic module recycling processes, Resour Conserv Recycl 187 (2022). https://doi.org/10.1016/j.resconrec.2022.106612.

[28] R.E. Russo, M. Awais, M. Fattobene, E. Santoni, R. Cavallera, S. Zamponi, P. Conti, M. Berrettoni, G. Giuli, Silver recovery from silicon solar cells waste by hydrometallurgical and electrochemical technique, Environ Technol Innov 36 (2024). https://doi.org/10.1016/j.eti.2024.103803.

[29] M. Khetri, M.C. Gupta, Recycling of silver from silicon solar cells by laser debonding, Solar Energy 270 (2024). https://doi.org/10.1016/j.solener.2024.112381.

[30] G. Zante, R. Marin Rivera, J.M. Hartley, A.P. Abbott, Efficient recycling of metals from solar cells using catalytic etchants, J Clean Prod 370 (2022). https://doi.org/10.1016/j.jclepro.2022.133552.

[31] C.E.L. Latunussa, F. Ardente, G.A. Blengini, L. Mancini, Life Cycle Assessment of an innovative recycling process for crystalline silicon photovoltaic panels, Solar Energy Materials and Solar Cells 156 (2016) 101–111. https://www.vdma.org/international-technology-roadmap-photovoltaic (accessed September 8, 2023).

[32] M. Tao, V. Fthenakis, B. Ebin, B. Steenari, E. Butler, P. Sinha, R. Corkish, K. Wambach, E.S. Simon, Major challenges and opportunities in silicon solar module recycling, Progress in Photovoltaics: Research and Applications 28 (2020) 1077–1088. https://doi.org/10.1002/pip.3316.

[33] IMARC, Metal Silicon Prices, Trend, Chart, Demand, Market Analysis, News, Historical and Forecast Data Report 2024 Edition, 2024. https://www.imarcgroup.com/metal-silicon-pricing-report (accessed October 17, 2024).

[34] Emiliano Bellini, Polysilicon price will stay above $5.50/kg for at least a year, PV Magazine (2024). https://www.pv-magazine.com/2024/04/16/polysilicon-price-will-stay-above-5-5-kg-for-at-least-a-year-says-analyst/ (accessed October 17, 2024).

[35] A. Derbouz Draoua, B. Martel, S. Dubois, C. Audoin, M. Sérasset, A. Fauveau, H.S. Radhakrishnan, J. Denafas, L. Petreniene, N. Severino, On the Fabrication of Solar Cells Based on Newly Produced Recycled Silicon Feedstocks From CABRISS-A Comparative Study Between Material Properties and Solar Cell Performances, in: EU PVSEC 2017-33rd European Photovoltaic Solar Energy Conference and Exhibition, WIP, 2017: pp. 483–487. https://doi.org/10.4229/EUPVSEC20172017-2AV.1.3.

[36] J.-K. Lee, S.-W. Ko, H.-M. Hwang, W.-G. Shin, Y.-C. Ju, G.-H. Kang, H.-E. Song, Y.-J. Eo, S. Bae, W. Palitzsch, Crystalline silicon solar cell with an efficiency of 20.05% remanufactured using 30% silicon scraps recycled from a waste photovoltaic module, Solar Energy Materials and Solar Cells 277 (2024) 113102. https://doi.org/10.1016/j.solmat.2024.113102.

[37] J. Park, N. Park, Wet etching processes for recycling crystalline silicon solar cells from end-of-life photovoltaic modules, RSC Adv 4 (2014) 34823–34829. https://doi.org/10.1039/C4RA03895A.

[38] J. Park, W. Kim, N. Cho, H. Lee, N. Park, An eco-friendly method for reclaimed silicon wafers from a photovoltaic module: from separation to cell fabrication, Green Chemistry 18 (2016) 1706–1714. https://doi.org/10.1039/C5GC01819F.

[39] W.-H. Huang, W.J. Shin, L. Wang, W.-C. Sun, M. Tao, Strategy and technology to recycle wafer-silicon solar modules, Solar Energy 144 (2017) 22–31. https://doi.org/10.1016/j.solener.2017.01.001.

[40] T.-Y. Wang, J.-C. Hsiao, C.-H. Du, Recycling of materials from silicon base solar cell module, in: 2012 38th IEEE Photovoltaic Specialists Conference, IEEE, 2012: pp. 2355–2358. https://doi.org/10.1109/PVSC.2012.6318071.

[41] S. Kang, S. Yoo, J. Lee, B. Boo, H. Ryu, Experimental investigations for recycling of silicon and glass from waste photovoltaic modules, Renew Energy 47 (2012) 152–159. https://doi.org/10.1016/j.renene.2012.04.030.

[42] B. Jung, J. Park, D. Seo, N. Park, Sustainable system for raw-metal recovery from crystalline silicon solar panels: from noble-metal extraction to lead removal, ACS Sustain Chem Eng 4 (2016) 4079–4083. https://doi.org/10.1021/acssuschemeng.6b00894.

[43] C. Latunussa, L. Mancini, G. Blengini, F. Ardente, D. Pennington, Analysis of material recovery from silicon photovoltaic panels, JRC Publications Repository JRC100783 (2016). https://doi.org/10.2788/786252.

[44] W.-H. Huang, W.J. Shin, L. Wang, W.-C. Sun, M. Tao, Strategy and technology to recycle wafer-silicon solar modules, Solar Energy 144 (2017) 22–31. https://doi.org/10.1016/j.solener.2017.01.001.

[45] N. Eshraghi, L. Berardo, A. Schrijnemakers, V. Delaval, M. Shaibani, M. Majumder, R. Cloots, B. Vertruyen, F. Boschini, A. Mahmoud, Recovery of nano-structured silicon from end-of-life photovoltaic wafers with value-added applications in lithium-ion battery, ACS Sustain Chem Eng 8 (2020) 5868–5879. https://doi.org/10.1021/acssuschemeng.9b07434.

[46] S. Yousef, M. Tatariants, J. Denafas, V. Makarevicius, S.-I. Lukošiūtė, J. Kruopienė, Sustainable industrial technology for recovery of Al nanocrystals, Si micro-particles and Ag from solar cell wafer production waste, Solar Energy Materials and Solar Cells 191 (2019) 493–501. https://doi.org/10.1016/j.solmat.2018.12.008.

[47] T. Dobra, D. Vollprecht, R. Pomberger, Thermal delamination of end-of-life crystalline silicon photovoltaic modules, Waste Management & Research 40 (2022) 96–103. https://doi.org/10.1177/0734242X211038184.

[48] J. Lee, J. Lee, Y. Ahn, G. Kang, H. Song, M. Kang, Y. Kim, C. Cho, Simple pretreatment processes for successful reclamation and remanufacturing of crystalline silicon solar cells, Progress in Photovoltaics: Research and Applications 26 (2018) 179–187. https://doi.org/10.1002/pip.2963.

[49] V. Fiandra, L. Sannino, C. Andreozzi, F. Corcelli, G. Graditi, Silicon photovoltaic modules at end-of-life: Removal of polymeric layers and separation of materials, Waste Management 87 (2019) 97–107. https://doi.org/10.1016/j.wasman.2019.02.004.

[50] V. Fiandra, L. Sannino, C. Andreozzi, G. Graditi, End-of-life of silicon PV panels: A sustainable materials recovery process, Waste Management 84 (2019) 91–101. https://doi.org/10.1016/j.wasman.2018.11.035.

[51] R. Deng, N. Chang, M.M. Lunardi, P. Dias, J. Bilbao, J. Ji, C.M. Chong, Remanufacturing end-of-life silicon photovoltaics: Feasibility and viability analysis, Progress in Photovoltaics: Research and Applications 29 (2021) 760–774. https://doi.org/10.1002/pip.3376.

[52] M. Tammaro, A. Salluzzo, J. Rimauro, S. Schiavo, S. Manzo, Experimental investigation to evaluate the potential environmental hazards of photovoltaic panels, J Hazard Mater 306 (2016) 395–405. https://doi.org/10.1016/j.jhazmat.2015.12.018.

[53] M. Tammaro, J. Rimauro, V. Fiandra, A. Salluzzo, Thermal treatment of waste photovoltaic module for recovery and recycling: Experimental assessment of the presence of metals in the gas emissions and in the ashes, Renew Energy 81 (2015) 103–112. https://doi.org/10.1016/j.renene.2015.03.014.

[54] S. Pang, Y. Yan, Z. Wang, D. Wang, S. Li, W. Ma, K. Wei, Enhanced separation of different layers in photovoltaic panel by microwave field, Solar Energy Materials and Solar Cells 230 (2021) 111213. https://doi.org/10.1016/j.solmat.2021.111213.

[55] Y. Kim, J. Lee, Dissolution of ethylene vinyl acetate in crystalline silicon PV modules using ultrasonic irradiation and organic solvent, Solar Energy Materials and Solar Cells 98 (2012) 317–322. https://doi.org/10.1016/j.solmat.2011.11.022.

[56] E.S. Lovato, L.M. Donato, P.P. Lopes, E.H. Tanabe, D.A. Bertuol, Application of supercritical CO2 for delaminating photovoltaic panels to recover valuable

materials, Journal of CO2 Utilization 46 (2021) 101477. https://doi.org/10.1016/j.jcou.2021.101477.

[57] X. Xu, D. Lai, G. Wang, Y. Wang, Nondestructive silicon wafer recovery by a novel method of solvothermal swelling coupled with thermal decomposition, Chemical Engineering Journal 418 (2021) 129457. https://doi.org/10.1016/j.cej.2021.129457.

[58] C. Libby, S. Shaw, G. Heath, K. Wambach, Photovoltaic recycling processes, in: 2018 IEEE 7th World Conference on Photovoltaic Energy Conversion (WCPEC)(A Joint Conference of 45th IEEE PVSC, 28th PVSEC & 34th EU PVSEC), IEEE, 2018: pp. 2594–2599. https://doi.org/10.1109/PVSC.2018.8547376.

[59] F. Pagnanelli, E. Moscardini, T. Abo Atia, L. Toro, Photovoltaic panel recycling: from type-selective processes to flexible apparatus for simultaneous treatment of different types, Mineral Processing and Extractive Metallurgy 125 (2016) 221–227. https://doi.org/10.1080/03719553.2016.1200764.

[60] P. Dias, L. Schmidt, L.B. Gomes, A. Bettanin, H. Veit, A.M. Bernardes, Recycling waste crystalline silicon photovoltaic modules by electrostatic separation, Journal of Sustainable Metallurgy 4 (2018) 176–186. https://doi.org/10.1007/s40831-018-0173-5.

[61] S. Kim, J. Kim, S. Cho, K. Seo, B.-U. Park, H.-S. Lee, J. Park, Development of eco-friendly pretreatment processes for high-purity silicon recovery from end-of-life photovoltaic modules, RSC Adv 14 (2024) 31451–31460. https://doi.org/10.1039/D4RA04878D.

[62] R. Frischknecht, K. Komoto, T. Doi, Life cycle assessment of crystalline silicon photovoltaic module delamination with hot knife technology, IEA PVPS Task 12, International Energy Agency Power Systems Programme, Report IEA-PVPS T12 (2023).

[63] M. Wahman, A. Surowiak, B. Ebin, K. Berent, PV back sheet recovery from c-Si modules using hot knife technique, Solar Energy Materials and Solar Cells 276 (2024) 113067. https://doi.org/10.1016/j.solmat.2024.113067.

[64] M. Ito, T. Doi, Recycling Technology Using Hot Knife Separation Method, in: 2024 31st International Workshop on Active-Matrix Flatpanel Displays and Devices (AM-FPD), IEEE, 2024: pp. 8–10. https://doi.org/10.23919/AM-FPD61635.2024.10615931.

[65] J.-H. Kim, J.-K. Lee, Y.-S. Ahn, J.-G. Yeo, J.-S. Lee, G.-H. Kang, C.-H. Cho, Peeling behavior of backsheet according to surface temperature of

photovoltaic module, Korean Journal of Materials Research 29 (2019) 703–708. https://doi.org/10.3740/MRSK.2019.29.11.703.

[66] R. Wang, E. Song, C. Zhang, X. Zhuang, E. Ma, J. Bai, W. Yuan, J. Wang, Pyrolysis-based separation mechanism for waste crystalline silicon photovoltaic modules by a two-stage heating treatment, RSC Adv 9 (2019) 18115–18123. https://doi.org/10.1039/C9RA03582F.

[67] Y. Akimoto, A. Iizuka, E. Shibata, High-voltage pulse crushing and physical separation of polycrystalline silicon photovoltaic panels, Miner Eng 125 (2018) 1–9. https://doi.org/10.1016/j.mineng.2018.05.015.

[68] B.-P. Song, M.-Y. Zhang, Y. Fan, L. Jiang, J. Kang, T.-T. Gou, C.-L. Zhang, N. Yang, G.-J. Zhang, X. Zhou, Recycling experimental investigation on end of life photovoltaic panels by application of high voltage fragmentation, Waste Management 101 (2020) 180–187. https://doi.org/10.1016/j.wasman.2019.10.015.

[69] P. Zhao, J. Guo, G. Yan, G. Zhu, X. Zhu, Z. Zhang, B. Zhang, A novel and efficient method for resources recycling in waste photovoltaic panels: High voltage pulse crushing, J Clean Prod 257 (2020) 120442. https://doi.org/10.1016/j.jclepro.2020.120442.

[70] S.-M. Nevala, J. Hamuyuni, T. Junnila, T. Sirviö, S. Eisert, B.P. Wilson, R. Serna-Guerrero, M. Lundström, Electro-hydraulic fragmentation vs conventional crushing of photovoltaic panels–Impact on recycling, Waste Management 87 (2019) 43–50. https://doi.org/10.1016/j.wasman.2019.01.039.

[71] P. Padhamnath, S. Nalluri, F. Kuśmierczyk, M. Kopyściański, J. Karbowniczek, S.W. Leow, T. Reindl, Electrohydraulic fragmentation processing enabling separation and recovery of all components in end-of-life silicon photovoltaic panels, Solar Energy 289 (2025) 113329. https://doi.org/https://doi.org/10.1016/j.solener.2025.113329.

[72] W. Kern, The evolution of silicon wafer cleaning technology, J Electrochem Soc 137 (1990) 1887. https://doi.org/10.1149/1.2086825.

[73] V. Shanmugam, A. Khanna, P.K. Basu, A.G. Aberle, T. Mueller, J. Wong, Impact of the phosphorus emitter doping profile on metal contact recombination of silicon wafer solar cells, Solar Energy Materials and Solar Cells 147 (2016) 171–176. https://doi.org/10.1016/j.solmat.2015.12.006.

[74] L. Liu, F. Lin, M. Heinrich, A.G. Aberle, B. Hoex, Unexpectedly high etching rate of highly doped n-type crystalline silicon in hydrofluoric acid, ECS

Journal of Solid State Science and Technology 2 (2013) P380. https://doi.org/10.1149/2.026309jss.

[75] H.F. Winters, D. Haarer, Influence of doping on the etching of Si (111), Phys Rev B 36 (1987) 6613. https://doi.org/10.1103/PhysRevB.36.6613.

[76] H. Seidel, L. Csepregi, A. Heuberger, H. Baumgärtel, Anisotropic etching of crystalline silicon in alkaline solutions: I. Orientation dependence and behavior of passivation layers, J Electrochem Soc 137 (1990) 3612. https://doi.org/10.1149/1.2086277.

[77] N. Moudir, Y. Boukennous, N. Moulaï-Mostefa, I. Bozetine, M. Maoudj, N. Kamel, Z. Kamel, D. Moudir, Preparation of silver powder used for solar cell paste by reduction process, Energy Procedia 36 (2013) 1184–1191. https://doi.org/10.1016/j.egypro.2013.07.134.

[78] M.M. Hilali, K. Nakayashiki, C. Khadilkar, R.C. Reedy, A. Rohatgi, A. Shaikh, S. Kim, S. Sridharan, Effect of Ag particle size in thick-film Ag paste on the electrical and physical properties of screen printed contacts and silicon solar cells, J Electrochem Soc 153 (2005) A5. https://doi.org/10.1149/1.2126579 DownloadArticle PDF.

[79] H.-C. Fang, C.-P. Liu, H.-S. Chung, C.-L. Huang, Effects of fine particle content in Al paste on screen printed contact formation and solar cell performance, J Electrochem Soc 157 (2010) H455. https://doi.org/10.1149/1.3314337.

[80] P. Padhamnath, J.K. Buatis, A. Khanna, N. Nampalli, N. Nandakumar, V. Shanmugam, A.G. Aberle, S. Duttagupta, Characterization of screen printed and fire-through contacts on LPCVD based passivating contacts in monoPoly™ solar cells, Solar Energy 202 (2020) 73–79. https://doi.org/10.1016/j.solener.2020.03.087.

[81] E. Bombach, I. Röver, A. Müller, S. Schlenker, K. Wambach, R. Kopecek, E. Wefringhaus, Technical experience during thermal and chemical recycling of a 23 year old PV generator formerly installed on Pellworm island, in: 21st European Photovoltaic Solar Energy Conference, Dresden, Germany, 2006: pp. 4–8.

[82] E. Klugmann-Radziemska, P. Ostrowski, Chemical treatment of crystalline silicon solar cells as a method of recovering pure silicon from photovoltaic modules, Renew Energy 35 (2010) 1751–1759. https://doi.org/10.1016/j.renene.2009.11.031.

[83] J.M. Howe, H.I. Aaronson, R. Gronsky, Atomic mechanisms of precipitate plate growth in the Al□ Ag system—I. Conventional transmission electron

microscopy, Acta Metallurgica 33 (1985) 639–648. https://doi.org/10.1016/0001-6160(85)90027-6.

[84] J.M. Howe, H.I. Aaronson, R. Gronsky, Atomic mechanisms of precipitate plate growth in the Al□Ag system—II. High-resolution transmission electron microscopy, Acta Metallurgica 33 (1985) 649–658. https://doi.org/10.1016/0001-6160(85)90028-8.

[85] Q. Hu, Z.X. Deng, L.B. Liu, L.G. Zhang, P.J. Masset, Experimental investigation of phase equilibria in the Al–Ag–Si system, Calphad 83 (2023) 102604. https://doi.org/10.1016/j.calphad.2023.102604.

[86] G.R. Armstrong, A. Hellawell, Composition and volume fraction changes in Ag-Al eutectic alloys, Acta Metallurgica 22 (1974) 1383–1389. https://doi.org/10.1016/0001-6160(74)90038-8.

[87] D.S. Pashkevich, A. V Mamaev, Production of hydrogen fluoride by processing fluorine-containing wastes and by-products of modern industries, WIT Transactions on Ecology and the Environment 231 (2019) 111–123.

[88] R. Wieland, M. Pittroff, J. Boudaden, S. Altmannshofer, C. Kutter, Environmental-friendly fluorine mixture for CVD cleaning processes to replace C2F6, CF4 and NF3, ECS Trans 72 (2016) 23. https://doi.org/10.1149/07219.0023ecst.

[89] J.B. Bulko, Production of High Value Fluorine Gases for the Semiconductor Industry, STARMET CORPORATION, Concord, MA (US), 2003. https://doi.org/10.2172/824744.

[90] A. Sanjurjo, L. Nanis, K. Sancier, R. Bartlett, V. Kapur, Silicon by sodium reduction of silicon tetrafluoride, J Electrochem Soc 128 (1981) 179. https://doi.org/10.1149/1.2127363.

[91] National Center for Biotechnology Information, PubChem Compound Summary for CID 24556, Silicon tetrafluoride., 2024 (n.d.). https://pubchem.ncbi.nlm.nih.gov/compound/Silicon-tetrafluoride. (accessed October 7, 2024).

[92] S.S. Abd El Rehim, H.H. Hassan, M.A.M. Ibrahim, M.A. Amin, Electrochemical behaviour of a silver electrode in NaOH solutions, Monatshefte Für Chemie/Chemical Monthly 129 (1998) 1103–1117.

[93] N. Iwasaki, Y. Sasaki, Y. Nishina, Ag electrode reaction in NaOH solution studied by in-situ Raman spectroscopy, Surf Sci 198 (1988) 524–540. https://doi.org/10.1016/0039-6028(88)90382-2.

[94] N. Iwasaki, Y. Sasaki, Y. Nishina, Raman spectral study of a Ag electrode in NaOH solution, Surf Sci 158 (1985) 352–358. https://doi.org/10.1016/0039-6028(85)90310-3.

[95] C.B. Porciúncula, N.R. Marcilio, I.C. Tessaro, M. Gerchmann, Production of hydrogen in the reaction between aluminum and water in the presence of NaOH and KOH, Brazilian Journal of Chemical Engineering 29 (2012) 337–348. https://doi.org/10.1590/S0104-66322012000200014.

[96] V. Testa, M. Gerardi, L. Zannini, M. Romagnoli, P.E. Santangelo, Hydrogen production from aluminum reaction with NaOH/H2O solution: Experiments and insight into reaction kinetics, Int J Hydrogen Energy 83 (2024) 589–603. https://doi.org/10.1016/j.ijhydene.2024.08.152.

[97] T. Hiraki, M. Takeuchi, M. Hisa, T. Akiyama, Hydrogen production from waste aluminum at different temperatures, with LCA, Mater Trans 46 (2005) 1052–1057. https://doi.org/10.2320/matertrans.46.1052.

[98] W.-S. Chen, Y.-J. Chen, K.-C. Yueh, C.-P. Cheng, T.-C. Chang, Recovery of valuable metal from Photovoltaic solar cells through extraction, in: IOP Conf Ser Mater Sci Eng, IOP Publishing, 2020: p. 012007. https://doi.org/10.1088/1757-899X/720/1/012007.

[99] F. Ardente, C.E.L. Latunussa, G.A. Blengini, Resource efficient recovery of critical and precious metals from waste silicon PV panel recycling, Waste Management 91 (2019) 156–167. https://doi.org/10.1016/j.wasman.2019.04.059.

[100] P. Dias, S. Javimczik, M. Benevit, H. Veit, A.M. Bernardes, Recycling WEEE: Extraction and concentration of silver from waste crystalline silicon photovoltaic modules, Waste Management 57 (2016) 220–225. https://doi.org/10.1016/j.wasman.2016.03.016.

[101] H. Kobayashi Asuha, O. Maida, M. Takahashi, H. Iwasa, Nitric acid oxidation of Si to form ultrathin silicon dioxide layers with a low leakage current density, J Appl Phys 94 (2003) 7328–7335. https://doi.org/10.1063/1.1621720.

[102] H. Kobayashi, K. Imamura, W.-B. Kim, S.-S. Im, Nitric acid oxidation of Si (NAOS) method for low temperature fabrication of SiO2/Si and SiO2/SiC structures, Appl Surf Sci 256 (2010) 5744–5756. https://doi.org/10.1016/j.apsusc.2010.03.092.

[103] K. Imamura, M. Takahashi, A. Asuha, Y. Hirayama, S. Imai, H. Kobayashi, Nitric acid oxidation of Si method at 120° C: HNO3 concentration dependence, J Appl Phys 107 (2010). https://doi.org/10.1063/1.3296395.

[104] A. Asuha, S. Imai, M. Takahashi, H. Kobayashi, Nitric acid oxidation of silicon at~ 120° C to form 3.5-nm SiO2/ Si structure with good electrical characteristics, Appl Phys Lett 85 (2004) 3783–3785. https://doi.org/10.1063/1.1804255.

[105] G. Thomassen, J. Dewulf, S. Van Passel, Prospective material and substance flow analysis of the end-of-life phase of crystalline silicon-based PV modules, Resour Conserv Recycl 176 (2022) 105917. https://doi.org/10.1016/j.resconrec.2021.105917.

[106] F.C. dos Santos Martins Padoan, P.G. Schiavi, G. Belardi, P. Altimari, A. Rubino, F. Pagnanelli, Material flux through an innovative recycling process treating different types of end-of-life photovoltaic panels: demonstration at pilot scale, Energies (Basel) 14 (2021) 5534. https://doi.org/10.3390/en14175534.

[107] J. Wang, Y. Feng, Y. He, The research progress on recycling and resource utilization of waste crystalline silicon photovoltaic modules, Solar Energy Materials and Solar Cells 270 (2024) 112804. https://doi.org/https://doi.org/10.1016/j.solmat.2024.112804.

[108] K. Agroui, A. Maallemi, M. Boumaour, G. Collins, M. Salama, Thermal stability of slow and fast cure EVA encapsulant material for photovoltaic module manufacturing process, Solar Energy Materials and Solar Cells 90 (2006) 2509–2514. https://doi.org/10.1016/j.solmat.2006.03.023.

[109] M.C.C. de Oliveira, A.S.A.D. Cardoso, M.M. Viana, V. de F.C. Lins, The causes and effects of degradation of encapsulant ethylene vinyl acetate copolymer (EVA) in crystalline silicon photovoltaic modules: A review, Renewable and Sustainable Energy Reviews 81 (2018) 2299–2317. https://doi.org/10.1016/j.rser.2017.06.039.

[110] U. Desai, B.K. Sharma, A. Singh, A. Singh, Improvement in the reliability of photovoltaic mini-modules through modifying the structural composition of EVA encapsulant, Solar Energy 242 (2022) 246–255. https://doi.org/10.1016/j.solener.2022.07.018.

[111] K.J. Lewis, Encapsulant material requirements for photovoltaic modules, in: ACS Publications, 1983. https://doi.org/10.1021/bk-1983-0220.ch023.

[112] W.S. Chen, Y.J. Chen, Y.A. Chen, The application of organic solvents and thermal process for eliminating EVA resin layer from waste photovoltaic modules, in: IOP Conf Ser Earth Environ Sci, IOP Publishing, 2019: p. 012012. https://doi.org/10.1088/1755-1315/291/1/012012.

[113] T. Doi, I. Tsuda, H. Unagida, A. Murata, K. Sakuta, K. Kurokawa, Experimental study on PV module recycling with organic solvent method, Solar Energy Materials and Solar Cells 67 (2001) 397–403. https://doi.org/10.1016/S0927-0248(00)00308-1.

[114] Y. Kim, J. Lee, Dissolution of ethylene vinyl acetate in crystalline silicon PV modules using ultrasonic irradiation and organic solvent, Solar Energy Materials and Solar Cells 98 (2012) 317–322. https://doi.org/10.1016/j.solmat.2011.11.022.

[115] P. Dias, P. Dias, H. Veit, Recycling crystalline silicon photovoltaic modules, Emerging Photovoltaic Materials: Silicon & Beyond (2018) 61–102. https://doi.org/10.1002/9781119407690.

[116] G.P. Karayannidis, D.S. Achilias, Chemical recycling of poly (ethylene terephthalate), Macromol Mater Eng 292 (2007) 128–146. https://doi.org/10.1021/ie960563c.

[117] P.K. Basu, D. Sarangi, M.B. Boreland, Single-component damage-etch process for improved texturization of monocrystalline silicon wafer solar cells, IEEE J Photovolt 3 (2013) 1222–1228. https://doi.org/10.1109/JPHOTOV.2013.2270357.

[118] M. Knausz, G. Oreski, G.C. Eder, Y. Voronko, B. Duscher, T. Koch, G. Pinter, K.A. Berger, Degradation of photovoltaic backsheets: Comparison of the aging induced changes on module and component level, J Appl Polym Sci 132 (2015). https://doi.org/10.1002/app.42093.

[119] M.D. Kempe, J.H. Wohlgemuth, Evaluation of temperature and humidity on PV module component degradation, in: 2013 IEEE 39th Photovoltaic Specialists Conference (PVSC), IEEE, 2013: pp. 120–125. https://doi.org/10.1109/PVSC.2013.6744112.

[120] J. Tracy, W. Gambogi, T. Felder, L. Garreau-Iles, H. Hu, T.J. Trout, R. Khatri, X. Ji, Y. Heta, K.R. Choudhury, Survey of material degradation in globally fielded PV modules, in: 2019 IEEE 46th Photovoltaic Specialists Conference (PVSC), IEEE, 2019: pp. 874–879. https://doi.org/10.1109/PVSC40753.2019.8981140.

[121] N. Kim, H. Kang, K.-J. Hwang, C. Han, W.S. Hong, D. Kim, E. Lyu, H. Kim, Study on the degradation of different types of backsheets used in PV module under accelerated conditions, Solar Energy Materials and Solar Cells 120 (2014) 543–548. https://doi.org/10.1016/j.solmat.2013.09.036.

[122] A. Omazic, G. Oreski, M. Halwachs, G.C. Eder, C. Hirschl, L. Neumaier, G. Pinter, M. Erceg, Relation between degradation of polymeric components in crystalline silicon PV module and climatic conditions: A literature review,

Solar Energy Materials and Solar Cells 192 (2019) 123–133. https://doi.org/10.1016/j.solmat.2018.12.027.

[123] A. Ndiaye, A. Charki, A. Kobi, C.M.F. Kébé, P.A. Ndiaye, V. Sambou, Degradations of silicon photovoltaic modules: A literature review, Solar Energy 96 (2013) 140–151. https://doi.org/10.1016/j.solener.2013.07.005.

[124] M. Aghaei, A. Fairbrother, A. Gok, S. Ahmad, S. Kazim, K. Lobato, G. Oreski, A. Reinders, J. Schmitz, M. Theelen, Review of degradation and failure phenomena in photovoltaic modules, Renewable and Sustainable Energy Reviews 159 (2022) 112160. https://doi.org/10.1016/j.rser.2022.112160.

[125] D. Wu, J. Zhu, T. Betts, R. Gottschalg, PV module degradation mechanisms under different environmental stress factors, (2012). repository.lboro.ac.uk (accessed March 6, 2025).

[126] W.O. Filtvedt, M. Javidi, A. Holt, M.C. Melaaen, E. Marstein, H. Tathgar, P.A. Ramachandran, Development of fluidized bed reactors for silicon production, Solar Energy Materials and Solar Cells 94 (2010) 1980–1995. https://doi.org/10.1016/j.solmat.2010.07.027.

[127] B. Ceccaroli, O. Lohne, E.J. Øvrelid, New advances in polysilicon processes correlating feedstock properties and good crystal and wafer performances, Physica Status Solidi (c) 9 (2012) 2062–2070. https://doi.org/10.1002/pssc.201100167.

[128] C. Wang, T. Wang, P. Li, Z. Wang, Recycling of SiCl4 in the manufacture of granular polysilicon in a fluidized bed reactor, Chemical Engineering Journal 220 (2013) 81–88. https://doi.org/10.1016/j.cej.2013.01.001.

[129] L.D. Crossman, J.A. Baker, Polysilicon technology, in: Semiconductor Silicon 1977, Electrochem. Soc Pennington, New Jersey, 1977: pp. 18–32.

[130] W. Zulehner, Czochralski growth of silicon, J Cryst Growth 65 (1983) 189–213. https://doi.org/10.1016/0022-0248(83)90051-9.

[131] P. Dold, Silicon crystallization technologies, in: Semiconductors and Semimetals, Elsevier, 2015: pp. 1–61. https://doi.org/10.1016/bs.semsem.2015.04.001.

[132] M. Tangstad, M. Ksiazek, V. Andersen, E. Ringdalen, Small scale laboratory experiments simulating an industrial silicon furnace, in: Proceedings of the Twelfth International Ferroalloys Congress, Sustainable Future, Helsinki, Finland, 2010: pp. 6–9.

[133] P. Padhamnath, M. Ślęzak, M. Karbowniczek, Disposing End of Life PV Modules – Reusing, Recycling and Upcycling, in: EU PVSEC 2023, EUPVSEC,

Lisbon, Portugal, 2023: pp. 001–008. https://doi.org/10.4229/EUPVSEC2023/5DV.2.62.

[134] L. Blaesing, A. Walnsch, S. Hippmann, C. Modrzynski, C. Weidlich, S. Pavón, M. Bertau, Ferrosilicon Production from Silicon Wafer Breakage and Red Mud, ACS Sustainable Resource Management 1 (2024) 404–416. https://doi.org/10.1021/acssusresmgt.3c00035.

[135] D. Sah, N.K. Upadhyay, S. Muthiah, S. Kumar, Growth and analysis of polycrystalline silicon ingots using recycled silicon from waste solar module, Solar Energy Materials and Solar Cells 261 (2023) 112524. https://doi.org/10.1016/j.solmat.2023.112524.

[136] L.J. Geerligs, A.D. Kuypers, M.J. Theelen, Potential for Recycled Silicon Solar Cells as Feedstock for New Ingot Growth, Progress in Photovoltaics: Research and Applications (2024). https://doi.org/10.1002/pip.3872.

[137] L.S.S. de Oliveira, M. Lima, L.H. Yamane, R.R. Siman, Silver recovery from end-of-life photovoltaic panels, Detritus 10 (2020) 62–74. https://doi.org/10.31025/2611-4135/2020.13939.

[138] Q. Han, Y. Gao, T. Su, J. Qin, C. Wang, Z. Qu, X. Wang, Hydrometallurgy recovery of copper, aluminum and silver from spent solar panels, J Environ Chem Eng 11 (2023) 109236. https://doi.org/10.1016/j.jece.2022.109236.

[139] S. Nieland, U. Neuhaus, T. Pfaff, E. Rädlein, New approaches for component recycling of crystalline solar modules, in: 2012 Electronics Goes Green 2012+, IEEE, 2012: pp. 1–5.

[140] Y.K. Yi, H.S. Kim, T. Tran, S.K. Hong, M.J. Kim, Recovering valuable metals from recycled photovoltaic modules, J Air Waste Manage Assoc 64 (2014) 797–807. https://doi.org/10.1080/10962247.2014.891540.

[141] C. Lei, B. Yan, T. Chen, X.-L. Wang, X.-M. Xiao, Silver leaching and recovery of valuable metals from magnetic tailings using chloride leaching, J Clean Prod 181 (2018) 408–415. https://doi.org/10.1016/j.jclepro.2018.01.243.

[142] L. Xiao, P. Han, Y. Wang, G. Fu, Z. Sun, S. Ye, Silver dissolution in a novel leaching system: Reaction kinetics study, International Journal of Minerals, Metallurgy, and Materials 26 (2019) 168–177. https://doi.org/10.1007/s12613-019-1721-0.

[143] S. Lee, B. Frimpong, S. Abbey, Y.S. Moon, K. Yoo, Y.-M. Oh, S.-K. Kim, S.-J. Kim, M.-W. Oh, Fabrication of conductive silver paste recovered from leaching of waste catalyst using hydrochloric acid, RSC Adv 12 (2022) 9698–9703. https://doi.org/10.1039/D1RA09435A.

[144] S. Yousef, M. Tatariants, J. Denafas, V. Makarevicius, S.-I. Lukošiūtė, J. Kruopienė, Sustainable industrial technology for recovery of Al nanocrystals, Si micro-particles and Ag from solar cell wafer production waste, Solar Energy Materials and Solar Cells 191 (2019) 493–501. https://doi.org/10.1016/j.solmat.2018.12.008.

[145] S. Kang, S. Yoo, J. Lee, B. Boo, H. Ryu, Experimental investigations for recycling of silicon and glass from waste photovoltaic modules, Renew Energy 47 (2012) 152–159. https://doi.org/10.1016/j.renene.2012.04.030.

[146] K. Treviño Rodríguez, A.I. Sánchez Vázquez, J.J. Ruiz Valdés, J. Ibarra Rodríguez, M.G. Paredes Figueroa, S. Porcar García, J.B. Carda Castelló, A. Álvarez Méndez, Photovoltaic Glass Waste Recycling in the Development of Glass Substrates for Photovoltaic Applications, Materials 16 (2023) 2848. https://doi.org/10.3390/ma16072848.

[147] P. Li, Y. Sun, Z. Hu, S. Li, J. Li, Y. Tan, Comprehensive recycling and utilization of photovoltaic waste: Use photovoltaic glass waste to refine silicon kerf waste, Sep Purif Technol 317 (2023) 123863. https://doi.org/10.1016/j.seppur.2023.123863.

[148] W. Palitzsch, U. Loser, Integrated PV-recycling-more efficient, more effective, in: 2017 IEEE 44th Photovoltaic Specialist Conference (PVSC), IEEE, 2017: pp. 2272–2274. https://doi.org/10.1109/PVSC.2017.8521517.

[149] M. Królikowski, M. Fotek, P. Żach, M. Michałowski, Development of a Recycling Process and Characterization of EVA, PVDF, and PET Polymers from End-of-Life PV Modules, Materials 17 (2024) 821. https://doi.org/10.3390/ma17040821.

[150] U.A. Yusufoglu, T.M. Pletzer, L.J. Koduvelikulathu, C. Comparotto, R. Kopecek, H. Kurz, Analysis of the annual performance of bifacial modules and optimization methods, IEEE J Photovolt 5 (2014) 320–328. https://doi.org/10.1109/JPHOTOV.2014.2364406.

[151] W. Mühleisen, J. Loeschnig, M. Feichtner, A.R. Burgers, E.E. Bende, S. Zamini, Y. Yerasimou, J. Kosel, C. Hirschl, G.E. Georghiou, Energy yield measurement of an elevated PV system on a white flat roof and a performance comparison of monofacial and bifacial modules, Renew Energy 170 (2021) 613–619. https://doi.org/10.1016/j.renene.2021.02.015.

[152] H.P. Yin, Y.F. Zhou, S.L. Sun, W.S. Tang, W. Shan, X.M. Huang, X.D. Shen, Optical enhanced effects on the electrical performance and energy yield of bifacial PV modules, Solar Energy 217 (2021) 245–252. https://doi.org/10.1016/j.solener.2021.02.004.

[153] X. Sun, M.R. Khan, C. Deline, M.A. Alam, Optimization and performance of bifacial solar modules: A global perspective, Appl Energy 212 (2018) 1601–1610. https://doi.org/10.1016/j.apenergy.2017.12.041.

[154] W. Gu, T. Ma, S. Ahmed, Y. Zhang, J. Peng, A comprehensive review and outlook of bifacial photovoltaic (bPV) technology, Energy Convers Manag 223 (2020) 113283. https://doi.org/10.1016/j.enconman.2020.113283.

[155] K. Anusuya, K. Vijayakumar, M.L.J. Martin, S. Manikandan, Agrophotovoltaics: enhancing solar land use efficiency for energy food water nexus, Renewable Energy Focus 50 (2024) 100600. https://doi.org/10.1016/j.ref.2024.100600.

[156] O.A. Katsikogiannis, H. Ziar, O. Isabella, Integration of bifacial photovoltaics in agrivoltaic systems: A synergistic design approach, Appl Energy 309 (2022) 118475. https://doi.org/10.1016/j.apenergy.2021.118475.

[157] G.M. Tina, F.B. Scavo, S. Aneli, A. Gagliano, Assessment of the electrical and thermal performances of building integrated bifacial photovoltaic modules, J Clean Prod 313 (2021) 127906. https://doi.org/10.1016/j.jclepro.2021.127906.

[158] M. Chen, W. Zhang, L. Xie, B. He, W. Wang, J. Li, Z. Li, Improvement of the electricity performance of bifacial PV module applied on the building envelope, Energy Build 238 (2021) 110849. https://doi.org/10.1016/j.enbuild.2021.110849.